Heavy neutral gauge bosons at the LHC in an extended MSSM

Gennaro Corcella [a,*], Simonetta Gentile [b,c]

[a] *INFN, Laboratori Nazionali di Frascati, Via E. Fermi 40, I-00044, Frascati, Italy*
[b] *Dipartimento di Fisica, Università di Roma 'La Sapienza', Roma, Italy*
[c] *INFN, Sezione di Roma, Piazzale A. Moro 2, I-00185, Roma, Italy*

Abstract

Searching for heavy neutral gauge bosons Z', predicted in extensions of the Standard Model based on a U(1)$'$ gauge symmetry, is one of the challenging objectives of the experiments carried out at the Large Hadron Collider. In this paper, we study Z' phenomenology at hadron colliders according to several U(1)$'$-based models and in the Sequential Standard Model. In particular, possible Z' decays into supersymmetric particles are included, in addition to the Standard Model modes so far investigated. We point out the impact of the U(1)$'$ group on the MSSM spectrum and, for a better understanding, we consider a few benchmarks points in the parameter space. We account for the D-term contribution, due to the breaking of U(1)$'$, to slepton and squark masses and investigate its effect on Z' decays into sfermions. Results on branching ratios and cross sections are presented, as a function of the MSSM and U(1)$'$ parameters, which are varied within suitable ranges. We pay special attention to final states with leptons and missing energy and make predictions on the number of events with sparticle production in Z' decays, for a few values of integrated luminosity and centre-of-mass energy of the LHC.

---

* Corresponding author.
  E-mail address: gennaro.corcella@lnf.infn.it (G. Corcella).

1. Introduction

The Standard Model (SM) of the strong and electroweak interactions has been so far successfully tested at several machines, such the LEP and Tevatron accelerators and has been lately confirmed by the data collected by the Large Hadron Collider (LHC). New physics models have nonetheless been proposed to solve the drawbacks of the SM, namely the hierarchy problem, the Dark Matter observation or the still undetected Higgs boson, responsible for the mass generation. The large amount of data collected at the centre-of-mass energy of 7 TeV at the LHC opens a window to extensively search for new physics. The further increase to 8 and ultimately 14 TeV, as well as higher integrated luminosities, will extend this investigation in the near future.

The simplest possible extension of the SM consists in a gauge group of larger rank involving the introduction of one extra $U(1)'$ factor, inspired by Grand Unification Theories (GUTs), which leads to the prediction of a new neutral gauge boson Z'. The phenomenology of the Z' has been studied from a theoretical viewpoint (see, e.g., the reviews [1,2] or the more recent work in Refs. [3,4]), whereas searches for new heavy gauge bosons have been carried out at the Tevatron by the CDF [5] and D0 [6] Collaborations and at the LHC by ATLAS [7] and CMS [8]. Besides the Z' bosons yielded by the extra $U(1)'$ group, the analyses have also investigated the so-called Sequential Standard Model (Z'_{SSM}), i.e. a Z' with the same couplings to fermions and gauge bosons as the Z of the SM. The Sequential Standard Model does not have theoretical bases like the $U(1)'$ models, but it is used as a benchmark, since, as will be seen later on, the production cross section is just function of the Z' mass and there is no dependence on other parameters.

The Tevatron analyses searched for high-mass dielectron resonances in $p\bar{p}$ collisions at 1.96 TeV and set a lower Z' mass limit of about 1023 (D0) and 963 (CDF) GeV for the Z'_{SSM}. The LHC experiments investigated the production of both dielectrons and dimuons at large invariant masses and several models of Z' production, i.e. different $U(1)'$ gauge groups. The CMS Collaboration, by using event samples corresponding to an integrated luminosity of 1.1 fb^{-1}, excluded a Z' with SM-like couplings and mass below 2.32 TeV, a GUT-inspired Z' below 1.49–1.69 TeV and a Kaluza–Klein graviton in extra-dimension models [9] below 0.71–1.63 TeV. The ATLAS Collaboration analyzed 5 fb^{-1} of data and obtained a bound of 2.21 TeV for the SM-like case, in the range 1.76–1.96 TeV for the $U(1)'$ scenarios and about 0.91–2.16 TeV for the Randall–Sundrum gravitons.[1]

All such analyses, and therefore the obtained exclusion limits, crucially rely on the assumption that the Z' decays into Standard Model particles, with branching ratios depending on its mass and, in the GUT-driven case, on the parameters characterizing the specific $U(1)'$ model: such a choice is dictated by the sake of minimizing the parameters ruling the Z' phenomenology. As a matter of fact, in the perspective of searching for new physics at the LHC, there is no actual reason to exclude Z' decays into channels beyond the SM, such as its supersymmetry. In fact, new physics contributions to the Z' width will significantly decrease the branching ratios into SM particles, and therefore the mass limits quoted by the experiments may have to be revisited. Furthermore, Z' decays into supersymmetric particles, if existing, represent an excellent tool to investigate the electroweak interactions at the LHC in a phase-space corner that cannot be

---

[1] The exclusion ranges depend on the specific $U(1)'$ model and, for the graviton searches, on the coupling value.

explored by employing the usual techniques. Therefore, the possible discovery of supersymmetry in Z' processes would open the road to additional investigations, since one would need to formulate a scenario accommodating both sparticles and heavy gauge bosons.

The scope of this paper is indeed the investigation of the phenomenology of Z' bosons at the LHC, assuming that they can decay into both SM and supersymmetric particles. As for supersymmetry, we shall refer to the Minimal Supersymmetric Standard Model (MSSM) [10,11] and study the dependence on the MSSM parameters. A pioneering study of supersymmetric contributions to Z' decays was carried out in [12], wherein the partial widths in all SM and MSSM channels were derived analytically, and the branching ratios computed for a few U(1)$'$ scenarios. However, the numerical analysis was performed for a mass $m_{Z'} = 700$ GeV, presently ruled out by the late experimental measurements, and only for one point of the supersymmetric phase space. Therefore, no firm conclusion could be drawn about the feasibility to search for the Z' within supersymmetry at the LHC. This issue was tackled again more recently. Ref. [13] studied how the Z' mass exclusion limits change once sparticle and exotic decay modes are included, for many U(1)$'$ models and varying the supersymmetric particle masses from 0 to 2.5 TeV. The Higgs and neutralino sectors in extensions of the MSSM, including GUT-inspired U(1)$'$ models, were thoroughly debated in [14] and [15], respectively. Ref. [16] considered the U(1)$'_{\text{B-L}}$ gauge group, B and L being the baryon and lepton numbers, and focused on the decay of the Z' into charged-slepton pairs for a few points in the MSSM phase space and various values of Z' and slepton masses. Ref. [17] investigated all possible decays of the Z' in the SM and MSSM, and several U(1)$'$ models, for two sets of supersymmetric parameters and a Z' mass in the 1–2 TeV range.

In the following, we shall extend the above work in several aspects. Special attention will be paid to the MSSM spectrum after the addition of the U(1)$'$ gauge symmetry. Squark and slepton masses will be parametrized as the sum of a soft mass and the so-called D- and F-terms [18]. In particular, accounting for the D-term has an impact on the sfermion masses, which get an extra contribution driven by the U(1)$'$ group. Higgs, chargino and neutralino masses will be determined by diagonalizing the corresponding mass matrices. A detailed study will be thereafter undertaken by allowing the U(1)$'$ and MSSM parameters to run within suitable ranges, taking into account the recent experimental limits. Throughout this work, particular care will be taken about the decay of the Z' into slepton pairs, i.e. charged sleptons or sneutrinos, eventually leading to final states with four charged leptons or two charged leptons and missing energy, due to neutralinos. In fact, in the complex hadronic environment of the LHC, leptonic final states are the best channels to perform precise measurements and searches. Slepton production in Z' decays has the advantage that the Z' mass is a further kinematical constrain on the invariant mass of the slepton pair. Moreover, the extension of the MSSM by means of the U(1)$'$ gauge group provides also an interesting scenario to study Dark Matter candidates, such as neutralinos [19,20] or right-handed sneutrinos [21], whose annihilation or scattering processes may proceed through the coupling with a Z' boson.

We shall present results for the Z' production cross sections and the branching ratios into both Standard Model and supersymmetric final states, thoroughly scanning the U(1)$'$ and MSSM parameter spaces, which will enable one to estimate the LHC event rates with sparticle production in Z' decays. We point out that, in order to draw a statement on the feasibility of the LHC to search for supersymmetry in Z' decays, one should also account for the Standard Model backgrounds. However, in assessing whether the signal can be separated from the background, one would need to consider exclusive final states, wherein acceptance cuts on final-state jets, leptons and possible missing energy, as well as detector effects, are expected to play a role. The

framework of a Monte Carlo generator [22,23], wherein both signal and background events are provided with parton showers, hadronization, underlying event and detector simulations, is therefore the ideal one to carry out such a comparison. We shall thus defer a detailed investigation of the backgrounds to a future study, after the implementation of our modelling for Z' production and decay in a Monte Carlo code.

The paper is organized as follows. In Section 2 we shall briefly discuss the $U(1)'$ gauge group yielding the Z' boson and the particle content of the MSSM. Section 3 will be devoted to summarize the new features of the MSSM, once it is used in conjunction with the $U(1)'$ group. In Section 4, as a case study, we will choose a specific point of the MSSM/$U(1)'$ parameter space, named 'Representative Point', and discuss the MSSM spectrum in this scenario. In Section 5, we shall present the Z' branching ratios into SM and BSM particles for several $U(1)'$ models and in the Sequential Standard Model. We will first investigate the decay rates in a particular 'Reference Point' of the parameter space and then vary the $U(1)'$ mixing angle and the MSSM parameters. Particular attention will be devoted to the decays into sleptons and to the dependence of the branching fractions on the slepton mass. In Section 6 the leading-order cross section for Z' production in the $U(1)'$ scenarios and in the Sequential Standard Model will be calculated. Besides, the number of events with sparticle production in Z' decays will be computed for a few energy and luminosity phases of the LHC. In Section 7 we shall summarize the main results of our study and make some final remarks on the future developments of the analysis here presented. In Appendix A the main formulas used to calculate the Z' branching ratios will be presented.

2. Modelling Z' production and decay

As discussed in the Introduction, we shall consider extensions of the Standard Model leading to Z' bosons, which will be allowed to decay into both SM and supersymmetric particles. For the sake of simplicity and minimizing the dependence of our analysis on unknown parameters, we shall refer to the MSSM. In this section we wish to briefly review the main aspects of the models used for Z' production and decay.

2.1. $U(1)'$ models and charges

There are several possible extensions of the SM that can be achieved by adding an extra $U(1)'$ gauge group, typical of string-inspired GUTs (see, e.g., Refs. [1,2] for a review): each model is characterized by the coupling constants, the breaking scale of $U(1)'$ and the scalar particle responsible for its breaking, the quantum numbers of fermions and bosons according to $U(1)'$. Throughout our work, we shall focus on the $U(1)'$ models explored by the experimental collaborations.

Among the $U(1)'$ gauge models, special care has been taken about those coming from a Grand Unification gauge group E_6, having rank 6, which breaks according to:

$$E_6 \rightarrow SO(10) \times U(1)'_\psi, \tag{1}$$

followed by

$$SO(10) \rightarrow SU(5) \times U(1)'_\chi. \tag{2}$$

The neutral vector bosons associated with the $U(1)'_\psi$ and $U(1)'_\chi$ groups are called Z'_ψ and Z'_χ, respectively. Any other model is characterized by an angle θ and leads to a Z' boson which can be expressed as[2]:

$$Z'(\theta) = Z'_\psi \cos\theta - Z'_\chi \sin\theta. \tag{3}$$

The orthogonal combination to Eq. (3) is supposed to be relevant only at the Planck scale and can therefore be neglected even at LHC energies. Another model, named $U(1)'_\eta$, is inherited by the direct breaking of E_6 to the Standard Model (SM) group, i.e. $SU(2)_L \times U(1)_Y$, as in superstring-inspired models:

$$E_6 \to SM \times U(1)'_\eta. \tag{4}$$

The yielded gauge boson is called Z'_η and corresponds to a mixing angle $\theta = \arccos\sqrt{5/8}$ in Eq. (3). The model orthogonal to $U(1)'_\eta$, i.e. $\theta = \arccos\sqrt{5/8} - \pi/2$, leads to a neutral boson which will be referred to as Z'_I. Furthermore, in the so-called secluded model, a $U(1)'_S$ model extends the MSSM with a singlet field S [24]. The connection with the E_6 groups is achieved assuming a mixing angle $\theta = \arctan(\sqrt{15}/9) - \pi/2$ and a gauge boson Z'_S.

In the Grand Unification group E_6 the matter superfields are included in the fundamental representation of dimension 27:

$$\mathbf{27} = \left(Q, u^c, e^c, L, d^c, \nu^c, H, D^c, H^c, D, S^c\right)_L. \tag{5}$$

In Eq. (5), Q is a doublet containing the left-handed quarks, i.e.

$$Q = \begin{pmatrix} u_L \\ d_L \end{pmatrix}, \tag{6}$$

whereas L includes the left-handed leptons:

$$L = \begin{pmatrix} \nu_L \\ e_L \end{pmatrix}. \tag{7}$$

In Eqs. (6) and (7), u, d and e denote generic quark and lepton flavours. Likewise, u_L^c, d_L^c, e_L^c and ν_L^c are singlets, which are conjugate to the left-handed fields and thus correspond to right-handed quarks and leptons.[3] In the case of supersymmetric extensions of the Standard Model, such as the MSSM, $Q, L, u_L^c, d_L^c, e_L^c$ and ν_L^c will be superfields containing also left-handed sfermions. Furthermore, in Eq. (5), H and H^c are colour-singlet, electroweak doublets which can be interpreted as Higgs pairs:

$$H = \begin{pmatrix} \phi_1^0 \\ \phi_1^- \end{pmatrix}, \qquad H^c = \begin{pmatrix} \phi_2^+ \\ \phi_2^0 \end{pmatrix}. \tag{8}$$

In the MSSM, H and H^c are superfields containing also the supersymmetric partners of the Higgs bosons, i.e. the fermionic higgsinos. Another possible description of the H and H^c fields in the representation **27** is that they consist of left-handed exotic leptons (sleptons) N and L, with the same SM quantum numbers as the Higgs fields in Eq. (8) [12].[4] Moreover, in Eq. (5),

---

[2] In Eq. (3) we followed the notation in [12] and we shall stick to it throughout this paper. One can easily recover the notation used in [1] by replacing $\theta \to \theta - \pi/2$.

[3] Following [18], the conjugate fields are related to the right-handed ones via relations like $u_L^c = u_R^\dagger$.

[4] In the assumption that H and H^c contain exotic leptons, it is: $H = \begin{pmatrix} N_L \\ E_L \end{pmatrix}$ and $H^c = \begin{pmatrix} E_L^c \\ N_L^c \end{pmatrix}$.

Table 1
Z' models along with the corresponding mixing angle, as given in Eq. (3).

Model	θ
Z'_ψ	0
Z'_χ	$-\pi/2$
Z'_η	$\arccos\sqrt{5/8}$
Z'_S	$\arctan(\sqrt{15}/9) - \pi/2$
Z'_I	$\arccos\sqrt{5/8} - \pi/2$
Z'_N	$\arctan\sqrt{15} - \pi/2$

D and D^c are exotic vector-like quarks (squarks) and S^c is a SM singlet.[5] In our phenomenological analysis, as well as in those performed in Refs. [12,16,17], leptons and quarks contained in the H and D fields are neglected and assumed to be too heavy to contribute to Z' phenomenology. We are nevertheless aware that this is a quite strong assumption and that in forthcoming BSM investigations one may well assume that such exotics leptons and quarks (sleptons and squarks) are lighter than the Z' and therefore they can contribute to Z' decays.

When E_6 breaks according to Eqs. (1) and (2), the fields in Eq. (5) are reorganized according to SO(10) and SU(5). The SU(5) representations are the following:

$$\mathbf{10} = (Q, u^c, e^c), \qquad \bar{\mathbf{5}} = (L, d^c), \qquad \mathbf{1} = (v^c), \qquad \bar{\mathbf{5}} = (H, D^c),$$
$$\mathbf{5} = (H^c, D), \qquad \mathbf{1} = (S^c). \tag{9}$$

From the point of view of SO(10), the assignment of the fields in the representations $\mathbf{16}$, $\mathbf{10}$ and $\mathbf{1}$ is not uniquely determined. In particular, there is no actual reason to decide which $\bar{\mathbf{5}}$ representation should be included in $\mathbf{16}$ rather than in $\mathbf{10}$. The usual assignment consists in having in the representation $\mathbf{16}$ the SM fermions and in the $\mathbf{10}$ the exotics:

$$\mathbf{16} = (Q, u^c, e^c, L, d^c, v^c), \qquad \mathbf{10} = (H, D^c, H^c, D), \qquad \mathbf{1} = (S^c). \tag{10}$$

An alternative description is instead achieved by including H and D^c in the $\mathbf{16}$, with L and d^c in the $\mathbf{10}$; this 'unconventional' E_6 scenario has been intensively studied in Refs. [25–27] and leads to a different Z' phenomenology. In our paper, we shall assume the 'conventional' SO(10) representations, as in Eq. (10). Nevertheless, it can be shown [27] that, given a mixing angle θ, the unconventional E_6 scenario can be recovered by applying the transformation:

$$\theta \to \theta + \arctan\sqrt{15}. \tag{11}$$

In fact, in our phenomenological analysis, we shall also consider the U(1)$'_N$ model leading to the so-called Z'_N boson, with a mixing angle $\theta = \arctan\sqrt{15} - \pi/2$. According to Eq. (11), the Z'_N model corresponds to the Z'_χ one, but in the unconventional E_6 scenario. Table 1 summarizes the U(1)$'$-based models which will be investigated throughout this paper, along with the values of the mixing angle θ.

---

[5] A variety of notation is in use in the literature to denote the exotic fields in the $\mathbf{27}$ representation. For example, in [2,25,26] the exotic quarks D and D^c are called h and h^c.

Table 2
U(1)$'$ charges of the fields in the representation 27 of the Grand Unification group E_6.

	$2\sqrt{10}Q'_\chi$	$2\sqrt{6}Q'_\psi$
Q	-1	1
u^c	-1	1
d^c	3	1
L	3	1
ℓ^c	-1	1
ν_ℓ^c	-5	1
H	-2	-2
H^c	2	-2
S^c	0	4
D	2	-2
D^c	-2	-2

The U(1)$'$ charges of the fields in Eq. (5), assuming that they are organized in the SO(10) representations as in (10), are listed in Table 2. Under a generic U(1)$'$ rotation, the charge of a field Φ is the following combination of the U(1)$'_\chi$ and U(1)$'_\psi$ charges:

$$Q'(\Phi) = Q'_\psi(\Phi)\cos\theta - Q'_\chi(\Phi)\sin\theta. \tag{12}$$

Besides the U(1)$'$ gauge groups, another model which is experimentally investigated is the so-called Sequential Standard Model (SSM), yielding a gauge boson Z'_{SSM}, heavier than the Z boson, but with the same couplings to fermions and gauge bosons as in the SM. As discussed in the Introduction, although the SSM is not based on strong theoretical arguments, studying the Z'_{SSM} phenomenology is very useful, since it depends only on one parameter, the Z' mass, and therefore it can set a benchmark for the U(1)$'$-based analyses.

In the following, the coupling constants of U(1)$_Y$, SU(2)$_L$ and U(1)$'$ will be named g_1, g_2 and g', respectively, with $g_1 = g_2 \tan\theta_W$, θ_W being the Weinberg angle. We shall also assume, as occurs in E_6-inspired models, a proportionality relation between the two U(1) couplings, as originally proposed in [28]:

$$g' = \sqrt{\frac{5}{3}} g_1. \tag{13}$$

Before closing this subsection, we wish to stress that, in general, the electroweak-interaction eigenstates Z and Z' mix to yield the mass eigenstates, usually labelled as Z_1 and Z_2. Ref. [29] addressed this issue by using precise electroweak data from several experiments and concluded that the mixing angle $\theta_{ZZ'}$ is very small for any Z' model, namely $\sin\theta_{ZZ'} \sim 10^{-3}$–$10^{-4}$. Likewise, even the ZZ' mixing associated with the extra kinetic terms due to the two U(1) groups is small and can be neglected [30].

2.2. Particle content of the Minimal Supersymmetric Standard Model

The Minimal Supersymmetric Standard Model (MSSM) is the most investigated scenario for supersymmetry, as it presents a limited set of new parameters and particle content with respect to the Standard Model. Above all, the MSSM contains the supersymmetric partners of the SM particles: scalar sfermions, such as sleptons $\tilde{\ell}^\pm$ and $\tilde{\nu}_\ell$ ($\ell = e, \mu, \tau$) and squarks $\tilde{q}$ ($q = u, d, c, s, t, b$), and fermionic gauginos, i.e. $\tilde{g}$, $\tilde{W}^\pm$, $\tilde{Z}$ and $\tilde{\gamma}$. It exhibits two Higgs doublets, which, after giving

mass to W and Z bosons, lead to five scalar degrees of freedom, usually parametrized in terms of two CP-even neutral scalars, h and H, with h lighter than H, one CP-odd neutral pseudoscalar A, and a pair of charged Higgs bosons $H^{\pm}$. Each Higgs has a supersymmetric fermionic partner, named higgsino. The light scalar Higgs, i.e. h, roughly corresponds to the SM Higgs.

The weak gauginos mix with the higgsinos to form the mass eigenstates: two pairs of charginos ($\tilde{\chi}_1^{\pm}$ and $\tilde{\chi}_2^{\pm}$) and four neutralinos ($\tilde{\chi}_1^0$, $\tilde{\chi}_2^0$, $\tilde{\chi}_3^0$ and $\tilde{\chi}_4^0$), where $\tilde{\chi}_1^0$ is the lightest and $\tilde{\chi}_4^0$ the heaviest. Particle masses and couplings in the MSSM are determined after diagonalizing the relevant mass matrices. Hereafter, we assume the conservation of R-parity, with the values $R_p = +1$ for SM particles and $R_p = -1$ for their supersymmetric partners. This implies the existence of a stable Lightest Supersymmetric Particle (LSP), present in any supersymmetric decay chain. The lightest neutralino, i.e. $\tilde{\chi}_1^0$, is often assumed to be the LSP.

As for the Higgs sector, besides the two Higgs doublets of the MSSM, the extra Z' requires another singlet Higgs to break the U(1)$'$ symmetry and give mass to the Z' itself. Moreover, two extra neutralinos are necessary, since one has a new neutral gaugino, i.e. the supersymmetric partner of the Z', and a further higgsino, associated with the above extra Higgs. As for the sfermions, squark and slepton masses will get an extra contribution to the so-called D-term, depending on the U(1)$'$ sfermion charges and Higgs vacuum expectation values. As will be discussed below, such D-terms, when summed to the soft masses and to the F-terms, will have a crucial impact on sfermion spectra and, whenever large and negative, they may even lead to discarding some MSSM/U(1)$'$ scenarios.

3. Extending the MSSM with the extra U(1)$'$ group

In our modelling of Z' production and decay into SM as well as supersymmetric particles, the phenomenological analysis in Ref. [12] will be further expanded and generalized. In this section we summarize a few relevant points which are important for our discussion, referring to the work in [12] for more details.

3.1. Higgs bosons in the MSSM and U(1)$'$ models

The two Higgs doublets predicted by the MSSM (Φ_1 and Φ_2) can be identified with the scalar components of the superfields H and H^c in Eq. (5), whereas the extra Higgs (Φ_3), necessary to break the U(1)$'$ symmetry and give mass to the Z', is associated with the scalar part of the singlet S^c. The three Higgs bosons are thus two weak-isospin doublets and one singlet:

$$\Phi_1 = \begin{pmatrix} \phi_1^0 \\ \phi_1^- \end{pmatrix}, \qquad \Phi_2 = \begin{pmatrix} \phi_2^+ \\ \phi_2^0 \end{pmatrix}, \qquad \Phi_3 = \phi_3^0.$$

The vacuum expectation values of the neutral Higgs bosons are given by $\langle \phi_i^0 \rangle = v_i/\sqrt{2}$, with $v_1 < v_2 < v_3$. From the Higgs vacuum expectation values, one obtains the MSSM parameter $\tan\beta$, i.e.

$$\tan\beta = v_2/v_1. \tag{14}$$

Hereafter, we shall denote the Higgs charges according to the U(1)$'$ symmetry as:

$$Q_1' = Q'(H), \qquad Q_2' = Q'(H^c), \qquad Q_3' = Q'(S^c). \tag{15}$$

Their values can be obtained using the numbers in Table 2 and Eq. (12).

The MSSM superpotential contains a Higgs coupling term giving rise to the well-known μ parameter; because of the extra field Φ_3, our model presents the additional contribution $W = \lambda \Phi_1 \Phi_2 \Phi_3$, leading to a trilinear scalar potential for the neutral Higgs bosons

$$V_\lambda = \lambda A_\lambda \phi_1^0 \phi_2^0 \phi_3^0. \tag{16}$$

The parameter λ in Eq. (16) is related to the usual μ term by means of the following relation, involving the vacuum expectation value of ϕ_3^0 [12]:

$$\mu = \frac{\lambda v_3}{\sqrt{2}}. \tag{17}$$

After symmetry breaking and giving mass to W, Z and Z' bosons, one is left with two charged ($H^\pm$), and four neutral Higgs bosons, i.e. one pseudoscalar A and three scalars h, H and H'.[6] Following [31], the charged-Higgs mass is obtained by diagonalizing the mass mixing matrix

$$\mathcal{M}_{H^\pm}^2 = \frac{1}{2} \begin{pmatrix} (g_2^2/2 - \lambda^2)v_1^2 + \lambda A_\lambda v_1 v_3/v_2 & (g_2^2/2 - \lambda^2)v_1 v_2 + \lambda A_\lambda v_3 \\ (g_2^2/2 - \lambda^2)v_1 v_2 + \lambda A_\lambda v_3 & (g_2^2/2 - \lambda^2)v_2^2 + \lambda A_\lambda v_2 v_3/v_1 \end{pmatrix} \tag{18}$$

and is given by

$$m_{H^\pm}^2 = \frac{\lambda A_\lambda v_3}{\sin 2\beta} + \left(1 - 2\frac{\lambda^2}{g_2^2}\right)m_W^2. \tag{19}$$

We refer to [12] for the mass matrix of the CP-even neutral Higgs bosons: the mass eigenvalues are to be evaluated numerically and cannot be expressed in closed analytical form. One can nonetheless anticipate that the mass of the heaviest H' is typically about the Z' mass, and therefore the Z' cannot decay into channels containing H'.

The mass of the pseudoscalar Higgs A is obtained after diagonalizing its 2×2 mass matrix and can be computed analytically, as done in [31]:

$$m_A^2 = \frac{\lambda A_\lambda v_3}{\sin 2\beta} \left(1 + \frac{v^2}{4v_3^2} \sin^2 2\beta\right), \tag{20}$$

where $v = \sqrt{v_1^2 + v_2^2}$.[7]

3.2. Neutralinos and charginos

Besides the four neutralinos of the MSSM, $\tilde{\chi}_1^0, \ldots, \tilde{\chi}_4^0$, two extra neutralinos are required, namely $\tilde{\chi}_5^0$ and $\tilde{\chi}_6^0$, associated with the Z' and with the new neutral Higgs breaking U(1)$'$. The 6×6 neutralino mass matrix is typically written in the basis of the supersymmetric neutral bosons $(-i\tilde{B}, -i\tilde{W}_3, -i\tilde{B}', \tilde{\Phi}_1, \tilde{\Phi}_2, \tilde{\Phi}_3)$. It depends on the Higgs vacuum expectation values, on the soft

---

[6] We point out that in [12] the three neutral Higgs bosons are denoted by H_i^0, with $i = 1, 2, 3$ and the pseudoscalar one by P^0.

[7] In Eqs. (19) and (20) we have fixed the typing mistakes contained in Ref. [12], wherein the expressions for the masses of charged and pseudoscalar Higgs bosons contain extra factors of 2.

masses of the gauginos $\tilde{B}$, $\tilde{W}_3$ and $\tilde{B}'$, named M_1, M_2 and M' hereafter, and on the Higgs $U(1)'$ charges Q_1', Q_2' and Q_3'. It reads:

$$\mathscr{M}_{\tilde{\chi}^0} = \begin{pmatrix} M_1 & 0 & 0 & -\frac{1}{2}g_1 v_1 & \frac{1}{2}g_1 v_2 & 0 \\ 0 & M_2 & 0 & \frac{1}{2}g_2 v_1 & \frac{1}{2}g_2 v_2 & 0 \\ 0 & 0 & M' & Q_1'g'v_1 & Q_2'g'v_2 & Q_3'g'v_3 \\ -\frac{1}{2}g_1 v_1 & \frac{1}{2}g_2 v_1 & Q_1'g'v_1 & 0 & \frac{1}{\sqrt{2}}\lambda v_3 & \frac{1}{\sqrt{2}}\lambda v_2 \\ \frac{1}{2}g_1 v_2 & -\frac{1}{2}g_2 v_2 & Q_2'g'v_2 & \frac{1}{\sqrt{2}}\lambda v_3 & 0 & \frac{1}{\sqrt{2}}\lambda v_1 \\ 0 & 0 & Q_3'g'v_3 & \frac{1}{\sqrt{2}}\lambda v_2 & \frac{1}{\sqrt{2}}\lambda v_1 & 0 \end{pmatrix}. \tag{21}$$

The neutralino mass eigenstates $(\tilde{\chi}_1^0, \ldots, \tilde{\chi}_6^0)$ and their masses are obtained numerically after diagonalizing the above matrix. Approximate analytic expressions for the neutrino masses, valid whenever M_1, M_2, M', v_1 and v_2 are much smaller than v_3, can be found in [32].

Since the new Z' and Higgs bosons are neutral, the chargino sector of the MSSM remains unchanged even after adding the extra $U(1)'$ group. The chargino mass matrix is given by [10]

$$\mathscr{M}_{\tilde{\chi}^\pm} = \begin{pmatrix} M_2 & \sqrt{2}m_W \sin\beta \\ \sqrt{2}m_W \cos\beta & -\mu \end{pmatrix} \tag{22}$$

and its eigenvalues are

$$m_{\tilde{\chi}_1^\pm, \tilde{\chi}_2^\pm}^2 = \frac{1}{2}\big[|M_2|^2 + |\mu|^2 + 2m_W^2 \mp \sqrt{\Delta_{\tilde{\chi}}}\big], \tag{23}$$

with

$$\Delta_{\tilde{\chi}} = \big(|M_2|^2 + |\mu|^2 + 2m_W^2\big)^2 - 4\big|\mu M_2 - m_W^2 \sin 2\beta\big|^2. \tag{24}$$

3.3. Sfermions

In principle, for the sake of a reliable determination of the sfermion masses, one would need to carry out a full investigation within models for supersymmetry breaking, such as gauge-, gravity- or anomaly-mediated mechanisms. Studying supersymmetry-breaking scenarios goes nevertheless beyond the scopes of the present work. We just point out that supersymmetry can be spontaneously broken if the so-called D-term and/or the F-term in the MSSM scalar potential have non-zero vacuum expectation values, which can be achieved by means of the Fayet–Iliopoulos [33] or O'Raifeartaigh [34] mechanisms, respectively.[8]

The sfermion squared masses can thus be expressed as the sum of a soft term m_0^2, often set to the same value for both squarks and sleptons at a given scale, and the corrections due to D- and F-terms [18]. The F-terms are proportional to the SM fermion masses and therefore they are mostly relevant for the stop quarks. The D-term can be, in principle, important for both light and heavy sfermions and, for the purpose our study, it consists of two contributions. A first term is a correction due to the hyperfine splitting driven by the electroweak symmetry breaking, already present in the MSSM. For a fermion a of weak isospin $T_{i,a}$, weak hypercharge Y_a and electric charge Q_a, this contribution to the D-term reads:

$$\Delta\tilde{m}_a^2 = \big(T_{3,a}g_1^2 - Y_a g_2^2\big)\big(v_1^2 - v_2^2\big) = \big(T_{3,a} - Q_a \sin^2\theta_W\big)m_Z^2 \cos 2\beta. \tag{25}$$

---

[8] The scalar potential is given, in terms of D- and F-terms, by $V(\phi, \phi^*) = F^{*i}F_i + D^a D_a/2$, with $D^a = -g_a(\phi^* T^a \phi)$ and $F_i = \delta W/\delta\phi_i$, where W is the superpotential, ϕ_i are the scalar (Higgs) fields, g_a and T^a the coupling constant and the generators of the gauge group of the theory.

A second contribution is due to possible extensions of the MSSM, such as our $U(1)'$ group, and is related to the Higgs bosons which break the new symmetry:

$$\Delta\tilde{m}_a'^2 = \frac{g'^2}{2} Q_a' \big(Q_1' v_1^2 + Q_2' v_2^2 + Q_3' v_3^2\big), \tag{26}$$

where Q_1', Q_2' and Q_3' are the Higgs $U(1)'$ charges defined in Eq. (15) and Q_a' the charge of sfermion a. When dealing with the Sequential Standard Model Z', only the first contribution to the D-term, Eq. (25), must be evaluated.

Left- and right-handed sfermions mix and therefore, in order to obtain the mass eigenstates, one needs to diagonalize the following squared mass matrix:

$$\mathcal{M}_{\tilde{f}}^2 = \begin{pmatrix} (M_{LL}^{\tilde{f}})^2 & (M_{LR}^{\tilde{f}})^2 \\ (M_{LR}^{\tilde{f}})^2 & (M_{RR}^{\tilde{f}})^2 \end{pmatrix}. \tag{27}$$

The value of the soft masses and the scale at which they are evaluated are in principle arbitrary, as long as the physical sfermion masses, obtained after diagonalizing the matrix (27), fall within the current experimental limits for slepton and squark searches. Following Ref. [12], we assume a common soft mass of the order of few TeV for all the sfermions at the Z' scale and add to it the D- and F-term contributions. Another possibility would be, as done e.g. in [18], fixing the soft mass at a high ultraviolet scale, such as the Planck mass, and then evolving it down to the typical energy of the process, by means of renormalization group equations.

As an example, we present the expression for the matrix elements in the case of an up-type squark:

$$\big(M_{LL}^{\tilde{u}}\big)^2 = \big(m_{\tilde{u}_L}^0\big)^2 + m_u^2 + \left(\frac{1}{2} - \frac{2}{3}x_w\right)m_Z^2\cos 2\beta + \Delta\tilde{m}_{\tilde{u}_L}'^2, \tag{28}$$

$$\big(M_{RR}^{\tilde{u}}\big)^2 = \big(m_{\tilde{u}_R}^0\big)^2 + m_u^2 + \left(\frac{1}{2} - \frac{2}{3}x_w\right)m_Z^2\cos 2\beta + \Delta\tilde{m}_{\tilde{u}_R}'^2, \tag{29}$$

$$\big(M_{LR}^{\tilde{u}}\big)^2 = m_u(A_u - \mu\cot\beta), \tag{30}$$

where $x_w = \sin^2\theta_W$, $m_{\tilde{u}_{L,R}}^0$ is the $\tilde{u}_{L,R}$ soft mass at the Z' energy scale and $A_f = m_u A_u$ is the coupling constant entering in the Higgs-sfermion interaction term.

The dependence on $m_{Z'}$ and on the mixing angle θ is embedded in the $\Delta\tilde{m}_{\tilde{u}_{L,R}}'^2$ term; analogous expressions hold for down squarks and sleptons [12]. In the following, the up-squark mass eigenstates will be named as $\tilde{u}_1$ and $\tilde{u}_2$ and their masses as $m_{\tilde{u}_1}$ and $m_{\tilde{u}_2}$. Likewise, $\tilde{d}_{1,2}$, $\tilde{\ell}_{1,2}$ and $\tilde{\nu}_{1,2}$ will be the mass eigenstates for down-type squarks, charged sleptons and sneutrinos and their masses will be denoted by $m_{\tilde{d}_{1,2}}$, $m_{\tilde{\ell}_{1,2}}$ and $m_{\tilde{\nu}_{1,2}}$, respectively.

The terms m_u^2 in Eqs. (28) and (29), as well as the mixing term (30) are inherited by the F-terms in the scalar potential. As the mass of SM light quarks and leptons is very small, such terms are typically irrelevant and the mass matrix of sleptons and light squarks is roughly diagonal. On the contrary, the mixing term M_{LR} can be relevant for top squarks, and therefore the stop mass eigenstates $\tilde{t}_{1,2}$ can in principle be different from the weak eigenstates $\tilde{t}_{L,R}$. However, we can anticipate that, as will be seen later on, for a Z' boson with a mass of the order of a few TeV, much higher than the top-quark mass, even the stop mixing term will be negligible.

4. Representative Point

The investigation on Z' production and decays into SM and BSM particles depends on several parameters, such as the Z' or supersymmetric particle masses; the experimental searches for physics beyond the Standard Model set exclusion limits on such quantities [35].

In the following, we shall first consider a specific configuration of the parameter space, which we call 'Representative Point', to study the Z' phenomenology in a scenario yielding non-zero branching ratios in the more relevant decay channels. Then, each parameter will be varied individually, in order to investigate its relevance on the physical quantities.

The set of parameters chosen is the following:

$$m_{Z'} = 3 \text{ TeV}, \qquad \theta = \arccos \sqrt{\frac{5}{8}} - \frac{\pi}{2},$$
$$\mu = 200, \qquad \tan\beta = 20, \qquad A_q = A_\ell = A_\lambda = A_f = 500 \text{ GeV},$$
$$m_{\tilde{q}_L}^0 = m_{\tilde{q}_R}^0 = m_{\tilde{\ell}_L}^0 = m_{\tilde{\ell}_R}^0 = m_{\tilde{\nu}_L}^0 = m_{\tilde{\nu}_R}^0 = 2.5 \text{ TeV},$$
$$M_1 = 100 \text{ GeV}, \qquad M_2 = 200 \text{ GeV}, \qquad M' = 1 \text{ TeV}, \tag{31}$$

where the value of θ corresponds to the Z'_I model and by q and ℓ we have denoted any possible quark and lepton flavour, respectively. In Eq. (31) the gaugino masses M_1 and M_2 satisfy, within very good accuracy, the following relation, inspired by Grand Unification Theories:

$$\frac{M_1}{M_2} = \frac{5}{3} \tan^2 \theta_W. \tag{32}$$

4.1. Sfermion masses

The sfermion masses are given by the sum of a common soft mass, which we have set to the same values for all squarks and sleptons at the Z' scale, as in Eq. (31), and the F- and D-terms, given in Eqs. (27)–(30). The D-term, and then the sfermion squared masses, is expected to depend strongly on the U(1)$'$ and MSSM parameters, and can possibly be negative and large, up to the point of leading to an unphysical (imaginary) sfermion mass. The F-term, being proportional to the lepton/quark masses, is significant only for top squarks. In Fig. 1 we study the dependence of squark (left) and slepton (right) masses on the U(1)$'$ mixing angle θ. The symbols $\tilde{u}_{1,2}\tilde{d}_{1,2}$, $\tilde{\ell}_{1,2}$ and $\tilde{\nu}_{1,2}$ stand for generic up-, down-type squarks, charged sleptons and sneutrinos, respectively. With the parametrization in Eq. (31), in particular the fact that the Z' mass has been fixed to 3 TeV, a value much higher than SM quark and lepton masses, the sfermion masses do not depend on the squark or slepton flavour. In this case, even the stop mixing term is negligible, so that the $\tilde{t}_{1,2}$ masses are roughly equal to those of the other up-type squarks.

In Fig. 1 the mass spectra are presented in the range $-1.2 < \theta < 0.8$: in fact, for $\theta < -1.2$ and $\theta > 0.8$ the squared masses of $\tilde{d}_2$ and $\tilde{\nu}_2$ become negative and thus unphysical, respectively, due to a D-term which is negative and large. This implies that the model Z'_χ, corresponding to $\theta = -\pi/2$, cannot be investigated within supersymmetry for the scenario in Eq. (31), as it does not yield a meaningful sfermion spectrum. In the following, we shall still investigate the phenomenology of the Z'_χ in a generic Two Higgs Doublet Model, but the sfermion decay modes will not contribute to its decay width. From Fig. 1 (left) one can learn that the masses of $\tilde{u}_1$ and $\tilde{d}_1$ are degenerate and vary from about 2.2 to 3 TeV for increasing values of θ, whereas the u_2 mass decreases from 2.7 to about 2 TeV. A stronger dependence on θ is exhibited by $m_{\tilde{d}_2}$: it is almost
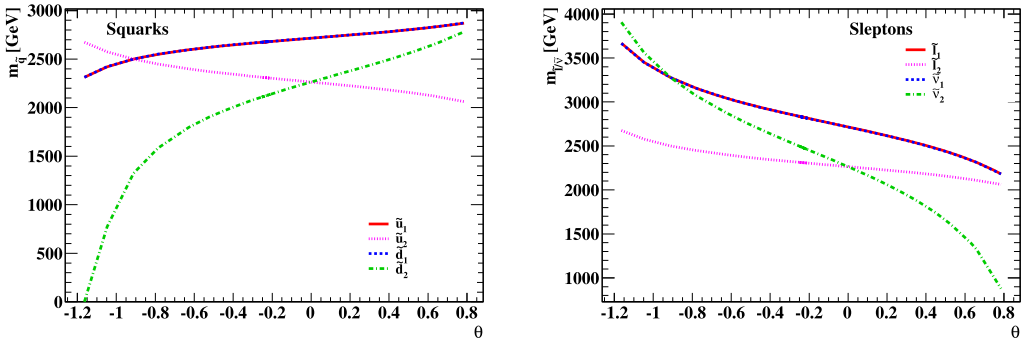
Fig. 1. Dependence on the U(1)′ mixing angle θ of squark (left) and slepton (right) masses.
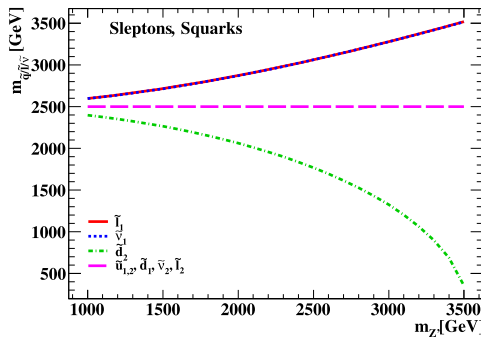

Fig. 2. Sfermion masses as a function of the Z' mass.

zero for $\theta \simeq -1.2$ and about 3 TeV for $\theta \simeq 0.8$. The slepton masses, as shown in Fig. 1 (right), decrease as θ increases: the mass of $\tilde{\ell}_1$ is degenerate with $\tilde{\nu}_1$ and shows a larger variation (from 3.7 to 2.2 TeV) than $\tilde{\ell}_2$ (from 2.7 to 2.2 TeV). Sneutrinos $\tilde{\nu}_2$ exhibit a remarkable θ dependence: $m_{\tilde{\nu}_2}$ can be as high as 4 TeV for $\theta \simeq -1.2$ and almost zero for $\theta \simeq 0.8$.

The D-term correction, and therefore the sfermion masses, is also function of the Z' mass: this dependence is studied for the Z'_I model and the parameters set as in the Representative Point, in the range 1 TeV $< m_{Z'} <$ 3.5 TeV. In Fig. 2 the squark and slepton masses are plotted with respect to $m_{Z'}$, obtaining quite cumbersome results. The masses of $\tilde{u}_{1,2}$, $\tilde{d}_1$, $\tilde{\ell}_2$ and $\tilde{\nu}_2$ are independent of m'_Z; on the contrary, $m_{\tilde{\nu}_1}$ and $m_{\tilde{\ell}_1}$ are degenerate and increase from 2.5 TeV ($m_{Z'} = 1$ TeV) to about 3.5 TeV ($m_{Z'} = 3.5$ TeV). The mass of $\tilde{d}_2$ is $m_{\tilde{d}_2} \simeq 2.4$ TeV for $m_{Z'} = 1$ TeV and $m_{\tilde{d}_2} \simeq 0$ for $m_{Z'} = 3.5$ TeV; due to the large negative D-term for $\tilde{d}_2$ squarks, no physical solution for $m_{\tilde{d}_2}$ is allowed above $m_{Z'} = 3.5$ TeV.

The dependence of the sfermion masses on the initial values $m_{\tilde{q}}^0$ and $m_{\tilde{\ell}}^0$, set at the Z' mass scale, and varied from 400 GeV to 4 TeV, is presented in Fig. 3. As expected, given Eqs. (28)–(30), all sfermion masses are monotonically increasing function of $m_{\tilde{f}}^0$; in the case of $\tilde{u}_1$, $\tilde{u}_2$, $\tilde{d}_1$ and ℓ_2, being the D-term negligible, they are degenerate and approximately equal to $m_{\tilde{\ell},\tilde{q}}^0$ in the whole explored range. The mass of the squark $\tilde{d}_2$ is instead physical only for $m_{\tilde{q}}^0 > 2.1$ TeV and increases up to the value $m_{\tilde{d}_2} \simeq 3.3$ TeV for $m_{\tilde{q}}^0 = 4$ TeV. The masses

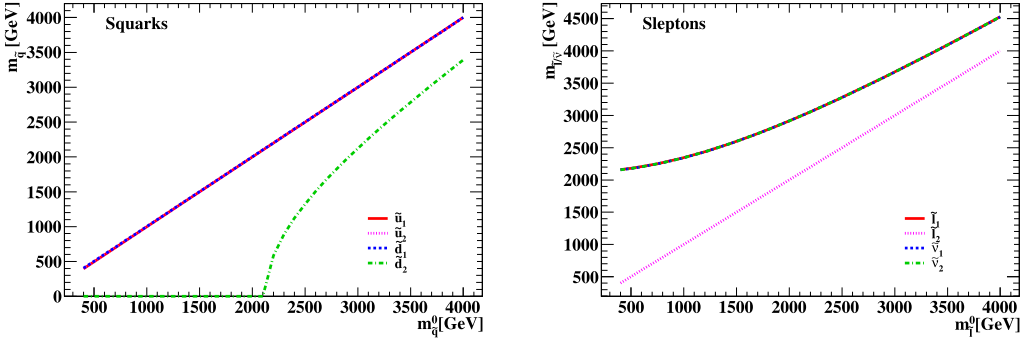Fig. 3. Sfermion masses as a function of the initial values $m_{\tilde{q}}^0$ and $m_{\tilde{\ell}}^0$, set at the Z' mass scale. Left: squarks. Right: sleptons.

Table 3
Neutralino masses for a Z' mass of 3 TeV and the parameters of the MSSM and U(1)$'$ set as in Eq. (31).

$m_{\tilde{\chi}_1^0}$	$m_{\tilde{\chi}_2^0}$	$m_{\tilde{\chi}_3^0}$	$m_{\tilde{\chi}_4^0}$	$m_{\tilde{\chi}_5^0}$	$m_{\tilde{\chi}_6^0}$
94.6 GeV	156.6 GeV	212.2 GeV	261.0 GeV	2541.0 GeV	3541.0 GeV

$m_{\tilde{\ell}_1}$, $m_{\tilde{\nu}_1}$ and $m_{\tilde{\nu}_2}$ are also degenerate and vary from about 2.1 TeV ($m_{\tilde{\ell}}^0 = 400$ GeV) to 4.5 TeV ($m_{\tilde{\ell}}^0 = 4$ TeV).

We also studied the variation of the sfermion masses with respect to $\tan\beta$, in the range $1.5 < \tan\beta < 5$, and on the trilinear coupling A_f, for 1 TeV $< A_f <$ 4 TeV, but found very little dependence on such parameters. Moreover, there is no dependence on M_1, M_2 and M', which do not enter in the expressions of the sfermion masses, even after the D-term correction.

4.2. Neutralino masses

We wish to study the dependence of the neutralino masses on the parameters playing a role in our analysis: unlike the sfermion masses, they depend also on the gaugino masses M_1, M_2 and M'. Table 3 reports the six neutralino masses for the parametrization in Eq. (31). For $m_{Z'} = 3$ TeV, Z' decays into channels containing the heaviest neutralino $\tilde{\chi}_6^0$ are not permitted because of phase-space restrictions, and therefore they can be discarded in the Representative Point scenario. Being $m_{\tilde{\chi}_5^0} \simeq 2.54$ TeV, decays into states containing $\tilde{\chi}_5^0$ are kinematically allowed, but one can already foresee very small branching ratios.

Fig. 4 presents the dependence of the mass of the four lightest neutralinos, i.e. $\tilde{\chi}_1^0, \ldots, \tilde{\chi}_4^0$, on the supersymmetry parameters μ (left) and $\tan\beta$ (right), for $-2000 < \mu < 2000$ and $1.5 < \tan\beta < 30$, with the others as in Eq. (31). The distribution of the masses of $\tilde{\chi}_1^0, \ldots, \tilde{\chi}_4^0$ is symmetric with respect to $\mu = 0$. Nevertheless, $m_{\tilde{\chi}_1^0}$ and $m_{\tilde{\chi}_2^0}$ increase from 0 ($\mu = 0$) to about 100 ($m_{\tilde{\chi}_1^0}$) and 200 GeV ($m_{\tilde{\chi}_2^0}$) in the range $|\mu| < 300$, whereas they are almost constant for $300 < |\mu| < 2000$. On the contrary, the masses of $\tilde{\chi}_3^0$ and $\tilde{\chi}_4^0$ exhibit a minimum for $\mu = 0$, about 110 and 230 GeV respectively, and increase monotonically in terms of $|\mu|$, with a behaviour leading to $m_{\tilde{\chi}_3^0} \sim m_{\tilde{\chi}_4^0} \sim |\mu|$ for large $|\mu|$. As for $\tan\beta$, a small dependence is visible only in the low $\tan\beta$ range, i.e. $1.5 < \tan\beta < 8$, with the masses of $\tilde{\chi}_1^0$, $\tilde{\chi}_2^0$ and $\tilde{\chi}_3^0$ slightly
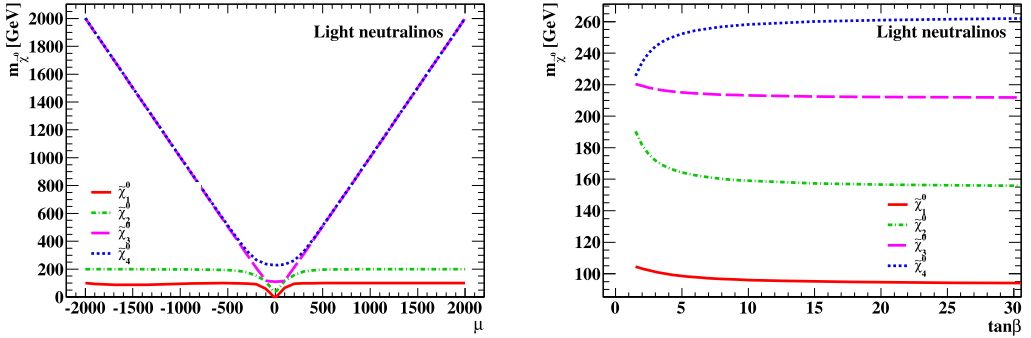
Fig. 4. Dependence of the mass of the four lightest neutralinos on the MSSM parameters μ (left) and $\tan \beta$ (right).
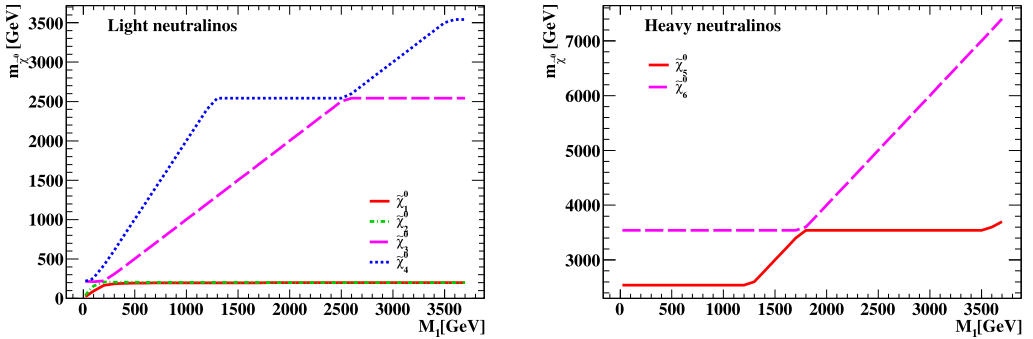

Fig. 5. Dependence of the neutralino masses on the MSSM parameter M_1. Left: light neutralinos. Right: heavy neutralinos.

decreasing and the one of $\tilde{\chi}_4^0$ mildly increasing. Outside this range, the light neutralino masses are roughly independent of $\tan \beta$.

In Fig. 5 we present the dependence of the light (left) and heavy (right) neutralino masses on the gaugino mass M_1 for $M_1 < 3.7$ TeV. In the light case, the masses exhibit a step-like behaviour: $m_{\tilde{\chi}_1^0}$ and $m_{\tilde{\chi}_2^0}$ have roughly the same value through all M_1 range, growing for small M_1 and amounting to approximately 200 GeV for $M_1 > 200$ GeV. The mass $m_{\tilde{\chi}_3^0}$ increases in the range 200 GeV $< M_1 < 2.5$ TeV and is about $m_{\tilde{\chi}_3^0} \simeq 2.54$ TeV for $M_1 > 2.5$ TeV. The mass of $\tilde{\chi}_4^0$ is roughly $m_{\tilde{\chi}_4^0} \simeq 2M_1$ for 200 GeV $< M_1 < 1.2$ TeV, then $m_{\tilde{\chi}_4^0} \simeq 2.54$ TeV, up to $M_1 \simeq 2.5$ TeV, and ultimately $m_{\tilde{\chi}_4^0} \simeq M_1$ for larger M_1. As for the heavy neutralinos, the mass of $\tilde{\chi}_5^0$ is $m_{\tilde{\chi}_5^0} \simeq 2.54$ TeV for $M_1 < 1.3$ TeV, then it increases linearly in the range 1.3 TeV $< M_1 < 1.8$ TeV and it is $m_{\tilde{\chi}_5^0} \simeq 3.54$ TeV for $M_1 > 1.8$ TeV. The mass of the heaviest neutralino $\tilde{\chi}_6^0$ is constant, namely $m_{\tilde{\chi}_6^0} \simeq 3.54$ TeV, for $M_1 < 1.8$ TeV, then it grows linearly, reaching the value $m_{\tilde{\chi}_6^0} \simeq 7$ TeV for $M_1 = 3.5$ TeV.

Fig. 6 presents the masses of $\tilde{\chi}_5^0$ and $\tilde{\chi}_6^0$ with respect to the Z' mass in the range 1 TeV $< m_{Z'} < 4$ TeV (left) and to the M' parameter for 100 GeV $< M' < 4$ TeV (right). The masses of $\tilde{\chi}_5^0$ and $\tilde{\chi}_6^0$ grow linearly as a function of $m_{Z'}$, whereas they exhibit opposite behaviour with
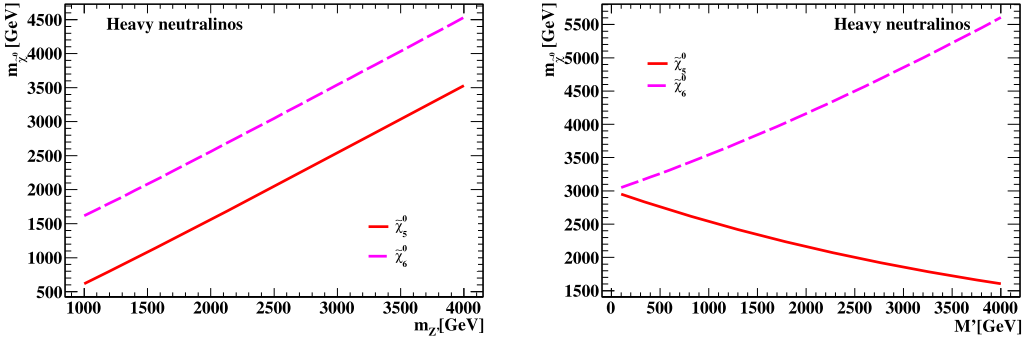
Fig. 6. Mass spectra of the heavy neutralinos as functions of the Z' mass (left) and the gaugino mass M' (right).
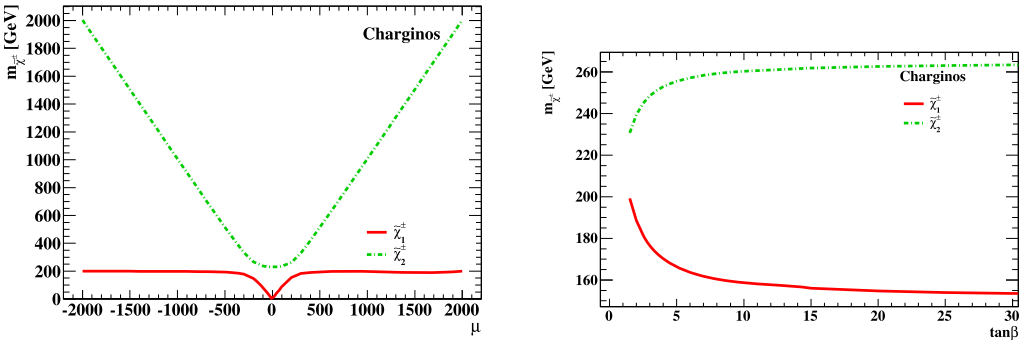
Fig. 7. Chargino masses with respect to the MSSM parameters μ (left) and $\tan\beta$ (right).

respect to M', as $m_{\tilde{\chi}_6^0}$ increases from 3 to 5.5 TeV and $m_{\tilde{\chi}_5^0}$ decreases from 3 to 1.5 TeV. The four light-neutralino masses are instead roughly independent of $m_{Z'}$ and M', as expected.

4.3. Chargino masses

As discussed before, the chargino sector remains unchanged after the introduction of the extra group U(1)$'$. Therefore, the chargino masses do not depend on the U(1)$'$ new parameter M' and on $m_{Z'}$, but just on the MSSM parameters μ, $\tan\beta$ and M_1. Figs. 7 and 8 show the dependence on such quantities, which are varied individually, with the other parameters fixed as in Eq. (31).

The dependence on μ, displayed in Fig. 7 (left), is symmetric with respect to $\mu = 0$. In particular, $m_{\tilde{\chi}_1^\pm}$ varies significantly, from about 3 to 200 GeV, only for $|\mu| < 300$, whereas the heavier chargino mass exhibits a behaviour $m_{\tilde{\chi}_1^\pm} \sim |\mu|$ and is as large as 2 TeV for $|\mu| \simeq 2000$. As for $\tan\beta$, Fig. 7 (right), the mass of the heavy chargino $\tilde{\chi}_2^\pm$ increases quite mildly from 230 to about 263 GeV, whereas $m_{\tilde{\chi}_1^\pm}$ decreases from almost 200 GeV ($\tan\beta = 1.5$) to about 154 GeV ($\tan\beta = 30$).

The variation with respect to M_1, presented in Fig. 8, is instead quite different for the two charginos. The mass of the lighter one changes very little only for $M_1 < 200$ GeV, whereas for larger M_1 it is about $m_{\tilde{\chi}_1^\pm} \simeq 200$ GeV. The mass of $\tilde{\chi}_2^\pm$ increases almost linearly with M_1 and is $m_{\chi_2^\pm} \simeq 2M_1 \simeq M_2$ for large M_1.
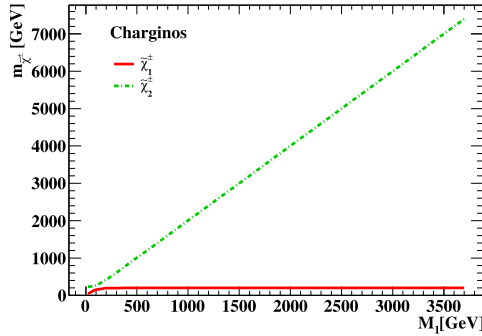
Fig. 8. Dependence of the chargino masses on the MSSM parameter M_1.
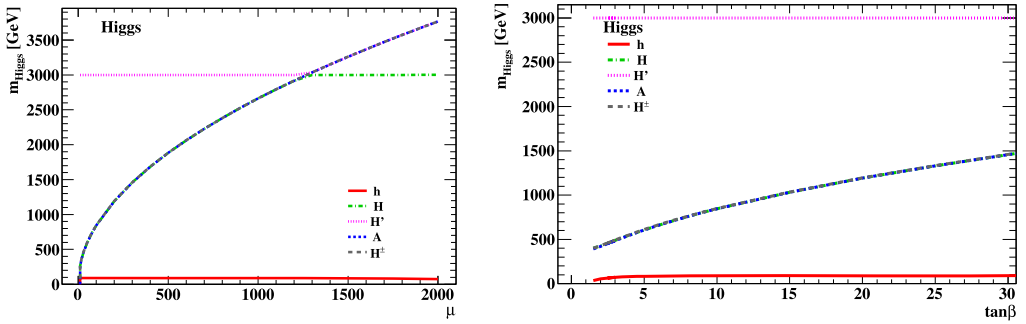
Fig. 9. Dependence of the mass of the Higgs bosons h, H, A, H' and $H^{\pm}$ on the MSSM quantities μ (left) and $\tan\beta$ (right).

4.4. Higgs masses

As pointed out before in the paper, after adding the $U(1)'$ symmetry, one has an extra neutral scalar Higgs, named H', besides the Higgs sector of the MSSM, i.e. the bosons h, H, $H^{\pm}$ and A. The Z' phenomenology will thus depend on the three Higgs masses and vacuum expectation values v_1, v_2 and v_3. In the Representative Point parametrization, the lightest h has a mass $m_h \simeq 90$ GeV, H, A and $H^{\pm}$ are degenerate and have a mass of about 1190 GeV, whereas the $U(1)'$-inherited H' is about 3 TeV, like the Z'. Therefore, in this scenario the Z' is not capable of decaying into final states containing H'.

Fig. 9 presents the variation of the Higgs masses in terms of μ (left) and $\tan\beta$ (right); Fig. 10 shows the dependence on $m_{Z'}$ (left) and A_f (right). One can immediately notice that the mass of the lightest h is roughly independent of these quantities and it is $m_h \simeq m_Z \simeq 90$ GeV through the whole μ, $\tan\beta$, $m_{Z'}$ and A_f ranges. Since the supersymmetric light Higgs h should roughly play the role of the SM Higgs boson, a value of about 90 GeV for its mass is too low, given the current limits from LEP [36] and Tevatron [37] experiments and the recent LHC results [38,39] on the observation of a new Higgs-like particle with a mass about 125 GeV. This is due to the fact that the h mass obtained after diagonalizing the neutral Higgs mass matrix is just a tree-level result; the possible inclusion of radiative corrections should increase the light Higgs mass value in such a way to be consistent with the experimental limits. In fact, the Representative Point will be used only to illustrate the features of the particle spectra in the MSSM, after one adds the extra
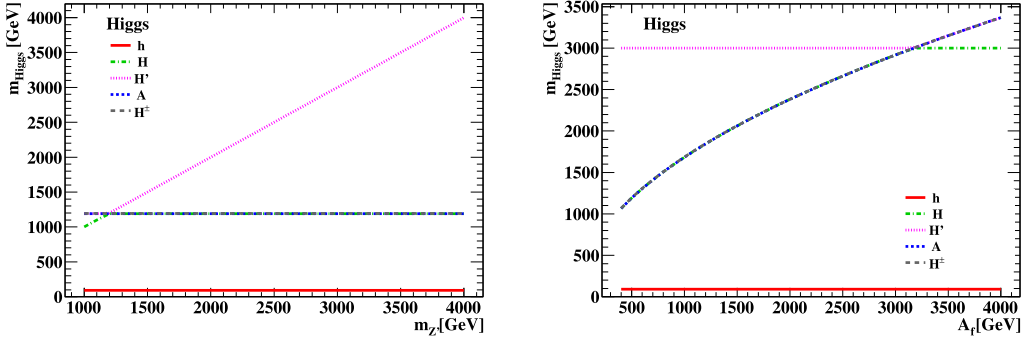
Fig. 10. Higgs mass spectra with respect to the Z' mass (left) and the trilinear coupling A_f (right).

U(1)$'$ symmetry group. Any realistic analysis of Z' decays in supersymmetry should of course use values of the Higgs masses accounting for higher-order corrections and in agreement with the experimental data.

The heavy MSSM scalar Higgs H is physical, i.e. its squared mass positive definite, only for positive values of μ, therefore in Fig. 9 the Higgs masses are plotted for $\mu > 0$. The mass of H increases monotonically from 0 ($\mu = 0$) to 3 TeV ($\mu \simeq 1260$), and then it is $m_H \simeq m_{Z'}$ also for larger μ-values. As for the U(1)$'$-inherited H', its mass is about $m_{H'} \simeq m_{Z'}$ for $0 < \mu < 1260$; for larger μ it increases monotonically, up to $m_{H'} \simeq 3.75$ TeV, value reached for $\mu = 2000$. In other words, for $\mu > 1260$, H and H' behave as if they exchanged their roles, with increasing $m_{H'}$ and constant $m_H = m_{Z'}$. The masses of A and $H^{\pm}$ exhibit instead the same behaviour and increase monotonically with respect to μ in the whole range. It is also interesting to notice that, for $0 < \mu < 1260$, one has $m_H \simeq m_{H^{\pm}} \simeq m_A$. As for the dependence on $\tan \beta$, presented in Fig. 9 (right), the masses of H, A and $H^{\pm}$ are almost degenerate and increase from about 400 GeV ($\tan \beta = 1.5$) to approximately 1.5 TeV ($\tan \beta = 30$). The mass of H' is instead $m_{H'} \simeq m_{Z'} = 3$ TeV for any value of $\tan \beta$.

The dependence of the Higgs masses on the Z' mass in the range 1 TeV $< m_{Z'} <$ 4 TeV is presented in Fig. 10 (left). A and $H^{\pm}$ are degenerate and their mass is constantly equal to 1.19 TeV in the whole explored region. The H mass is $m_H \simeq 1$ TeV for $m_{Z'} = 1$ TeV, then it slightly increases and amounts to $m_H \simeq 1.19$ TeV in the range 1.2 TeV $< m_{Z'} <$ 4 TeV. Fig. 10 (right) shows the Higgs masses as functions of the trilinear coupling A_f for 500 GeV $< A_f <$ 4 TeV. The masses of the charged and pseudoscalar Higgs bosons are degenerate and increase from 1.1 TeV ($A_f = 500$ GeV) to about 3.4 TeV ($A_f = 4$ TeV). The mass of the scalar neutral H is degenerate with the ones of A and $H^{\pm}$ for 500 GeV $< A_f <$ 3.2 TeV, then it is $m_H = m_{Z'} = 3$ TeV for A_f between 3.2 and 4 TeV. The H' mass is constant, i.e. $m_{H'} = m_{Z'} = 3$ TeV for 500 GeV $< A_f <$ 3.2 TeV, then it increases in the same manner as the masses of $H^{\pm}$ and A. As already observed for the μ dependence, H and H' exchange their roles for $A_f > 3.2$ TeV.

4.5. Consistency of the MSSM masses with ISAJET

An experimental search for supersymmetric Z' decays demands the implementation of our MSSM/U(1)$'$ scenario in a Monte Carlo event generator. Therefore, it is essential to verify whether our mass spectra are consistent with those provided by the codes typically used to compute masses and decay rates in supersymmetry. For this purpose, a widely used program is the

Table 4
Mass values in GeV for neutralinos, charginos and Higgs bosons in our model, based on U(1)$'$ and the MSSM, and according to the ISAJET code, which implements only the MSSM.

Model	$m_{\tilde{\chi}_1^0}$	$m_{\tilde{\chi}_2^0}$	$m_{\tilde{\chi}_3^0}$	$m_{\tilde{\chi}_4^0}$	m_h	m_H	m_A	$m_{H^\pm}$	$m_{\tilde{\chi}_1^\pm}$	$m_{\tilde{\chi}_2^\pm}$
U(1)$'$/MSSM	94.6	156.6	212.2	261.0	90.7	1190.0	1190.0	1190.0	155.0	263.0
MSSM	91.3	152.2	210.2	266.7	114.1	1190.0	1197.9	1200.7	147.5	266.8

ISAJET package [40], containing all the MSSM data; the supersymmetric particle masses and branching ratios obtained by running ISAJET are then used by programs, such as HERWIG [22] and PYTHIA [23], which simulate hard scattering, parton showers, hadronization and underlying event, for an assigned MSSM configuration. It is thus crucial assessing whether such an approach can still be employed even after the inclusion of the extra Z' boson. Squark and slepton masses, corrected by the D-term contribution, can be directly given as an input to ISAJET. Moreover, the chargino spectrum is unchanged, being the Z' neutral, whereas the extra H', being too heavy, is not relevant for the Z' phenomenology. Besides, the masses of the MSSM Higgs bosons h, H, A and $H^\pm$ depend very mildly on the U(1)$'$ parameters. In the neutralino sector, the two additional $\tilde{\chi}_5^0$ and $\tilde{\chi}_6^0$ are also too heavy to be phenomenologically relevant. However, the neutralino mass matrix, Eq. (21), depends also on extra new parameters, such as M', g' and the U(1)$'$ charges $Q'_{1,2,3}$. Therefore, even the mass of the four light neutralinos can potentially feel the effect of the presence of the Z'.

We quote in Table 4 the eigenvalues of the neutralino mass matrix, Eq. (21), along with the masses yielded by ISAJET, for the parameter configuration corresponding to the Representative Point, Eq. (31). For the sake of completeness, we also present the Higgs and chargino mass values obtained in our framework (U(1)$'$ and MSSM), to investigate whether they agree with the ISAJET results (only MSSM).

From Table 4 one learns that the masses of the neutralinos agree within 5%; a larger discrepancy is instead found, about 20%, for the mass of the lightest Higgs, i.e. h; as pointed out before, this difference is due to the fact that, unlike ISAJET, our calculation is just a tree-level one and does not include radiative corrections. Both Higgs masses are nevertheless much smaller than the $m_{Z'}$, fixed to 3 TeV in the Representative Point; therefore, Z' decays into Higgs bosons will not be significantly affected by this discrepancy.

As for the chargino masses, the difference between our analytical calculation and the prediction of ISAJET is approximately 5% for $\tilde{\chi}_1^\pm$ and 1% for $\tilde{\chi}_2^\pm$. Overall, one can say that some differences in the spectra yielded by our computations and ISAJET are visible, but they should not have much impact on Z' phenomenology. The implementation of the U(1)$'$ model in HERWIG or PYTHIA, along with the employment of a standalone program like ISAJET for masses and branching ratios in supersymmetry, may thus provide a useful tool to explore Z' phenomenology in an extended MSSM.

4.6. Z' decays in the Representative Point

Before concluding this section, we wish to present the branching ratios of the Z' boson into both SM and new-physics particles. If BSM decays are competitive with the SM ones, then the current limits on the Z' mass will have to be reconsidered. We shall first present the branching ratios in the Representative Point parametrization, Eq. (31), i.e. a Z'_1 boson with mass 3 TeV, and then we will vary the quantities entering in our analysis.

Table 5
Masses in GeV of BSM particles in the MSSM/U(1)′ scenario, with the parameters set as in Eq. (31).

$m_{\tilde{u}_1}$	$m_{\tilde{u}_2}$	$m_{\tilde{d}_1}$	$m_{\tilde{d}_2}$	$m_{\tilde{\ell}_1}$	$m_{\tilde{\ell}_2}$	$m_{\tilde{\nu}_1}$	$m_{\tilde{\nu}_2}$
2499.4	2499.7	2500.7	1323.1	3279.0	2500.4	3278.1	3279.1

$m_{\tilde{\chi}_1^0}$	$m_{\tilde{\chi}_2^0}$	$m_{\tilde{\chi}_3^0}$	$m_{\tilde{\chi}_4^0}$	$m_{\tilde{\chi}_5^0}$	$m_{\tilde{\chi}_6^0}$	$m_{\tilde{\chi}_1^\pm}$	$m_{\tilde{\chi}_2^\pm}$
94.6	156.5	212.2	260.9	2541.4	3541.4	154.8	262.1

m_h	m_A	m_H	$m_{H'}$	$m_{H^\pm}$
90.7	1190.7	1190.7	3000.0	1193.4

4.6.1. Branching ratios in the Representative Point

In Table 5 we summarize, for the reader's convenience, the masses of the BSM particles for the parameters in Eq. (31), in such a way to figure out the decay channels which are kinematically permitted. At this point it is possible to calculate the Z' widths into the kinematically allowed decay channels. The Z' SM decay channels are the same as the Z boson, i.e. quark or lepton pairs, with the addition of the W^+W^- mode, which is accessible due to the higher Z' mass. However, since the Z' has no direct coupling to W bosons, the $Z' \to W^+W^-$ occurs only via ZZ' mixing and therefore one can already foresee small branching ratios. Furthermore, the extended MSSM allows Z' decays into squarks, i.e. $\tilde{q}_i \tilde{q}_i^*$ ($q = u, d$ and $i = 1, 2$), charged sleptons $\tilde{\ell}_i \tilde{\ell}_i$, sneutrinos $\tilde{\nu}_{i,\ell} \tilde{\nu}_{i,\ell}^*$ ($\ell = e, \mu, \tau, i = 1, 2$), neutralino, chargino, or Higgs ($hh, HH, hH, hA, HA, H'A, H^+H^-$) pairs, as well as into states with Higgs bosons associated with W/Z, such as Zh, ZH and $W^\pm H^\mp$.

We refer to [12] for the analytical form of such widths, at leading order in the U(1)′ coupling constant, i.e. $\mathcal{O}(g'^2)$; in Appendix A the main formulas will be summarized. Summing up all partial rates, one can thus obtain the Z' total width and the branching ratios into the allowed decay channels.

In Table 6 we quote the Z' branching ratios in the Representative Point parametrization. Since, at the scale of 3 TeV, one does not distinguish the quark or lepton flavour, the quoted branching ratios are summed over all possible flavours and $u\bar{u}$, $d\bar{d}$, $\ell^+\ell^-$ and $\nu\bar{\nu}$ denote any possible up-, down-type quark, charged-lepton or neutrino pair. Likewise, $\tilde{u}\tilde{u}^*$, $\tilde{d}\tilde{d}^*$, $\tilde{\ell}^+\tilde{\ell}^-$ and $\tilde{\nu}\tilde{\nu}^*$ are their supersymmetric counterparts. We present separately the branching ratios into all possible different species of charginos and neutralinos, as they yield different decay chains and final-state configurations. In Table 6, several branching ratios are zero or very small: the decays into up-type squarks and sleptons, heavy neutralinos $\tilde{\chi}_6^0$ and the U(1)′-inherited H' are kinematically forbidden for a Z' of 3 TeV. The only allowed decay into sfermion pairs is the one into down-type squarks $\tilde{d}_2\tilde{d}_2^*$. Despite being kinematically permitted, the width into up-type quarks vanishes, since, as will be clarified in Appendix A, in the Z_I' model the vector (v_u) and vector-axial (a_u) couplings, contained in the in the interaction Lagrangian of the Z' with up quarks, are zero. From Table 6 we learn that, at the Representative Point, the SM decays account for roughly the 77% of the total Z' width and the BSM ones for the remaining 23%. As for the BSM modes, the rate into down squarks is about 9% of the total rate, the ones into charginos and neutralinos 4.2% and 8.4%, respectively. In the gaugino sector, the channels $\tilde{\chi}_2^0\tilde{\chi}_3^0$ and $\tilde{\chi}_1^\pm\tilde{\chi}_2^\mp$ have the highest branching ratios. The decay into $\tilde{\chi}_1^0\tilde{\chi}_1^0$ has a very small branching fraction and is experimentally undetectable if $\tilde{\chi}_1^0$ is the lightest supersymmetric particle (LSP). The final states with Higgs bosons are characterized by very small rates: the branching fractions into H^+H^- and HA are

Table 6

Branching ratios of the Z' with the parameters fixed as in Eq. (31). The branching ratios into fermions and sfermions have been summed over all the possible flavours, e.g. $u\bar{u}$ ($\ell^+\ell^-$) denotes the sum of the rates into up, charm and top (electron, muon and tau) pairs.

Final state	BR (%)	Final state	BR (%)
$u\bar{u}$	0.00	$\tilde{\chi}_1^0 \tilde{\chi}_1^0$	0.07
$d\bar{d}$	40.67	$\tilde{\chi}_1^0 \tilde{\chi}_2^0$	0.43
$\ell^+\ell^-$	13.56	$\tilde{\chi}_1^0 \tilde{\chi}_3^0$	0.71
$\nu\bar{\nu}$	27.11	$\tilde{\chi}_1^0 \tilde{\chi}_4^0$	0.27
$\tilde{u}\tilde{u}^*$	0.00	$\tilde{\chi}_1^0 \tilde{\chi}_5^0$	$\mathscr{O}(10^{-6})$
$\tilde{d}\tilde{d}^*$	9.58	$\tilde{\chi}_2^0 \tilde{\chi}_2^0$	0.65
$\tilde{\ell}^+\tilde{\ell}^-$	0.00	$\tilde{\chi}_2^0 \tilde{\chi}_3^0$	2.13
$\tilde{\nu}\tilde{\nu}^*$	0.00	$\tilde{\chi}_2^0 \tilde{\chi}_4^0$	0.80
W^+W^-	$\mathscr{O}(10^{-5})$	$\tilde{\chi}_2^0 \tilde{\chi}_5^0$	$\mathscr{O}(10^{-6})$
H^+H^-	0.50	$\tilde{\chi}_3^0 \tilde{\chi}_3^0$	1.75
hA	$\mathscr{O}(10^{-3})$	$\tilde{\chi}_3^0 \tilde{\chi}_4^0$	1.31
HA	0.51	$\tilde{\chi}_3^0 \tilde{\chi}_5^0$	$\mathscr{O}(10^{-6})$
ZH	$\mathscr{O}(10^{-3})$	$\tilde{\chi}_4^0 \tilde{\chi}_4^0$	0.25
Zh	$\mathscr{O}(10^{-5})$	$\tilde{\chi}_4^0 \tilde{\chi}_5^0$	$\mathscr{O}(10^{-7})$
ZH'	0.00	$\tilde{\chi}_5^0 \tilde{\chi}_5^0$	0.00
$H'A$	0.00	$\sum_i \tilde{\chi}_i^0 \tilde{\chi}_6^0$	0.00
$W^\pm H^\mp$	$\mathscr{O}(10^{-3})$	$\tilde{\chi}_1^+ \tilde{\chi}_1^-$	1.76
		$\tilde{\chi}_1^\pm \tilde{\chi}_2^\mp$	1.95
		$\tilde{\chi}_2^+ \tilde{\chi}_2^-$	0.54

about 0.5%, the one into $H^\pm W^\mp$ roughly 0.1% and an even lower rate, $\mathscr{O}(10^{-7})$, is yielded by the modes hZ, ZH and hA.

These considerations, obtained in the particular configuration of the Reference Point, Eq. (31), can be extended to a more general context. We can then conclude that the Z' BSM branching fractions are not negligible and should be taken into account in the evaluation of the mass limits.

4.6.2. Parameter dependence of the branching ratios

In this subsection we wish to investigate how the Z' branching fractions into SM and supersymmetric particles fare with respect to the U(1)$'$ and MSSM parameters. As in Section 3, the study will be carried out at the Representative Point, varying each parameter individually.

In Fig. 11, the dependence of the branching ratios on the mixing angle θ is presented for SM (left) and BSM (right) decay modes, in the range $-1 < \theta < 0.8$; for the SM channels, we have also plotted the total branching ratio. The Z' decay rate into quarks exhibits a quite flat distribution, amounting to about 40% for central values of θ and slightly decreasing for large $|\theta|$. The branching ratio into neutrino pairs is enhanced for θ at the edges of the explored range, being about 25%, and presents a minimum for $\theta \simeq -0.1$. The rate into charged leptons varies between 5 and 15%, with a small enhancement around $|\theta| \simeq 0.8$; the branching fraction into W^+W^- is below 2% in the whole θ range.

As for the BSM channels, described in Fig. 11 (right), the neutralino, chargino, and Higgs modes have a similar behaviour, with a central broad maximum around $\theta = 0$ and branching
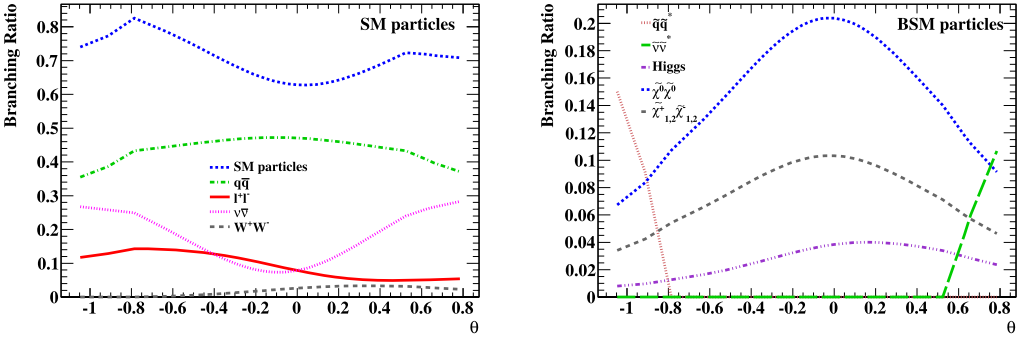
Fig. 11. Dependence of the Z' decay rates on the U(1)$'$ mixing angle θ. Left: SM modes; right: BSM channels.
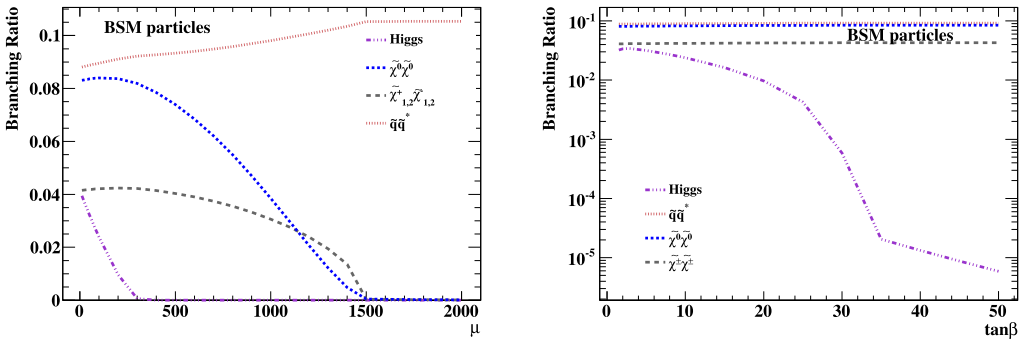
Fig. 12. BSM branching ratios with respect to the MSSM parameters μ (left) and $\tan\beta$ (right).

ratios about 20%, 10% and 3%, respectively The sneutrino modes give a non-negligible contribution only for $\theta > 0.5$, reaching about 10%, at the boundary of the investigated θ region, i.e. $\theta \simeq 0.8$. The squark-pair channel has a significant rate, about 15%, for negative mixing angles, i.e. $\theta \simeq = -1$. The rates in the Higgs channels lie between the neutralino and chargino ones and exhibit a maximum value, about 10%, for $\theta = 0$.

Fig. 12 presents the dependence of the BSM Z' branching ratios on the MSSM parameters μ (left) and $\tan\beta$ (right). The SM rates are not shown, since their dependence on these parameters is negligible. The decay rate into squarks slightly increases from 9 to 10% in the explored μ range; the neutralino branching ratio decreases quite rapidly from about 8% ($\mu = 0$) to zero ($\mu \simeq 1500$). The rate into charginos is about 4% for small values of μ, then it smoothly decreases, being negligible for $\mu > 1500$. The branching fraction into Higgs modes is almost 4% at $\mu = 0$ and rapidly becomes nearly zero for $\mu > 300$. As for $\tan\beta$, the $\tilde{q}\tilde{q}^*$, $\tilde{\chi}^+\tilde{\chi}^-$ and $\tilde{\chi}^0\tilde{\chi}^0$ modes are roughly independent of it, with rates about 9% (squarks), 8% (neutralinos) and 4% (charginos). The decays into states with Higgs bosons account for 4% of the Z' width at small $\tan\beta$ and are below 1% for $\tan\beta > 20$.

5. Z' decays into final states with leptons

Leptonic final states are considered as golden channels from the viewpoint of the LHC experimental searches. To exploit these features, this study will be focused on the decays of the Z'
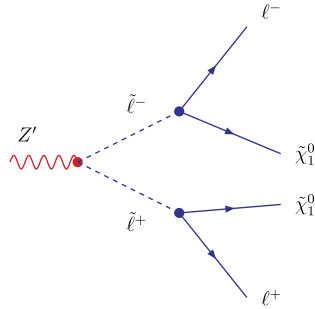
Fig. 13. Diagram for the decay of the Z' into a charged-slepton pair, yielding a final state with two charged leptons and missing energy.
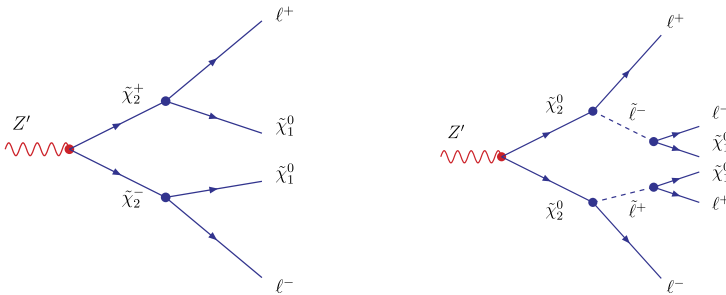
Fig. 14. Decays of Z' bosons into chargino (left) and neutralino (right) pairs, leading to final states with two charged leptons and missing energy.

boson into supersymmetric particles, leading to final states with leptons and missing energy, due to the presence of neutralinos or neutrinos. Final states with two charged leptons and missing energy come from primary decays $Z' \to \tilde{\ell}^+ \tilde{\ell}^-$, presented in Fig. 13, with the charged sleptons decaying into a lepton and a neutralino.

Furthermore, an analogous final state results from primary decays into charginos $Z' \to \tilde{\chi}_2^+ \tilde{\chi}_2^-$, followed by $\tilde{\chi}_2^\pm \to \ell^\pm \tilde{\chi}_1^0$, as in Fig. 14 (left). With respect to the direct production in pp collisions, where the partonic centre-of-mass energy is not uniquely determined, the production of charginos in Z' decays has the advantage that the Z' mass sets a kinematic constrain on the chargino invariant mass.

A decay chain, leading to four charged leptons and missing energy, is yielded by Z' decays into neutralinos $Z' \to \tilde{\chi}_2^0 \tilde{\chi}_2^0$, with subsequent $\tilde{\chi}_2^0 \to \ell^\pm \tilde{\ell}^\mp$ and $\tilde{\ell}^\pm \to \ell^\pm \tilde{\chi}_1^0$, as in Fig. 14 (right). Finally, we shall also investigate the decay into sneutrino pairs, such as $Z' \to \tilde{\nu}_2 \tilde{\nu}_2^*$, followed by $\tilde{\nu}_2 \to \tilde{\chi}_2^0 \nu$ and $\tilde{\chi}_2^0 \to \ell^+ \ell^- \tilde{\chi}_1^0$, with an intermediate charged slepton (see Fig. 15). The final state of the latest decay chain is made of four charged leptons plus missing energy, due to neutrinos and neutralinos. In the following, we wish to present a study of Z' decays into leptonic final states for a given set of the MSSM and U(1)$'$ parameters. In particular, we shall be interested in understanding the behaviour of such rates as a function of the slepton mass, which will be treated as a free parameter. In order to increase the rate into sleptons, with respect to the scenario yielded by the Representative Point, the squark mass at the Z' scale will be increased to 5 TeV, in such a way to suppress Z' decays into hadronic jets.

In our study we consider the models in Table 1 and vary the initial slepton mass $m_{\tilde{\ell}}^0$ for several fixed values of $m_{Z'}$, with the goal of determining an optimal combination of $m_{\tilde{\ell}}^0$ and $m_{Z'}$,
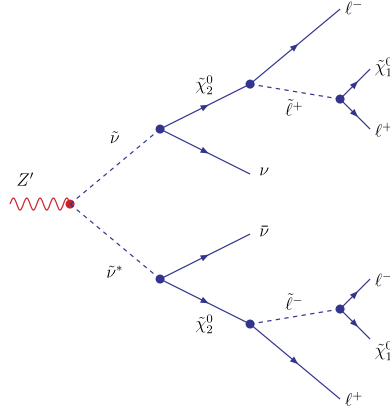
Fig. 15. Final state with four charged leptons and missing energy, due to the presence of neutrinos and neutralinos, yielded by a primary $Z' \to \tilde{\nu}\tilde{\nu}^*$ decay.

enhancing the rates into leptonic final states, i.e. the decay modes containing primary sleptons, charginos or neutralinos. The other parameters are set to the following Reference Point:

$$\mu = 200, \qquad \tan\beta = 20, \qquad A_q = A_\ell = A_f = 500 \text{ GeV},$$
$$m_{\tilde{q}}^0 = 5 \text{ TeV}, \qquad M_1 = 150 \text{ GeV}, \qquad M_2 = 300 \text{ GeV}, \qquad M' = 1 \text{ TeV}. \qquad (33)$$

Any given parametrization will be taken into account only if the sfermion masses are physical after the addition of the D-term. Hereafter, we denote by $\text{BR}_{q\bar{q}}$, $\text{BR}_{\ell^+\ell^-}$, $\text{BR}_{\nu\bar{\nu}}$ and $\text{BR}_{W^+W^-}$ the branching ratios into quark, charged-lepton, neutrino and W pairs, with BR_{SM} being the total SM decay rate. Likewise, $\text{BR}_{\tilde{q}\tilde{q}^*}$, $\text{BR}_{\tilde{\ell}^+\tilde{\ell}^-}$ and $\text{BR}_{\tilde{\nu}\tilde{\nu}^*}$ are the rates into squarks, charged sleptons and sneutrinos, $\text{BR}_{\tilde{\chi}^+\tilde{\chi}^-}$, $\text{BR}_{\tilde{\chi}^0\tilde{\chi}^0}$, $\text{BR}_{H^+H^-}$, BR_{hA}, BR_{HA} are the ones into chargino, neutralino, charged- and neutral-Higgs pairs, $\text{BR}_{W^\mp H^\pm}$ the branching fraction into $W^\mp H^\pm$. Moreover, for convenience, BR_{Zh} is the sum of the branching ratios into Zh and ZH and BR_{BSM} the total BSM branching ratio.

5.1. Reference Point: Model Z'_η

An extra U(1)$'$ group with a mixing angle $\theta = \arccos\sqrt{5/8}$ leads to a new neutral boson labelled as Z'_η. In Table 7 we list the masses of charged ($m_{\tilde{\ell}_1}$ and $m_{\tilde{\ell}_2}$) and neutral ($m_{\tilde{\nu}_1}$ and $m_{\tilde{\nu}_2}$) sleptons, for various $m_{Z'}$ and for the values of $m_{\tilde{\ell}}^0$ which, as will be clarified later, yield a physical sfermion spectrum and a maximum and minimum rate into sneutrinos. From Table 7 we learn that the decays into pairs of charged sleptons are always kinematically forbidden, whereas the decay into $\tilde{\nu}_2$ pairs is accessible. The effect of the D-term on the mass of $\tilde{\nu}_2$ is remarkable: variations of $m_{\tilde{\ell}}^0$ of few hundreds GeV induce in $m_{\tilde{\nu}_2}$ a change of 1 TeV or more, especially for large values of the Z' mass. Table 8 summarizes the branching ratios into all allowed SM and BSM channels, for the same $m_{Z'}$ and $m_{\tilde{\ell}}^0$ values as in Table 7, whereas Fig. 16 presents the branching ratio $Z'_\eta \to \tilde{\nu}_2\tilde{\nu}_2^*$ as a function of $m_{\tilde{\ell}}^0$ and for 1 TeV $< m_{Z'} <$ 4 TeV. The branching fraction into sneutrinos can be as large as about 11% for any value of $m_{Z'}$; for larger $m_{\tilde{\ell}}^0$ the sneutrino rate decreases, as displayed in Fig. 16. Furthermore, Table 8 shows that, within the scenario identified by the Reference Point, even the decays into charginos and neutralinos are

Table 7

Slepton masses at the Reference Point for the Z'_η model, varying $m_{Z'}$ and $m^0_{\tilde{\ell}}$. $m_{\tilde{\ell}_{1,2}}$ and $m_{\tilde{\nu}_{1,2}}$ are the charged-slepton and sneutrino mass eigenvalues, as discussed in the text. All masses are given in GeV.

$m_{Z'}$	$m^0_{\tilde{\ell}}$	$m_{\tilde{\ell}_1}$	$m_{\tilde{\ell}_2}$	$m_{\tilde{\nu}_1}$	$m_{\tilde{\nu}_2}$
1000	800	736.9	665.9	732.6	379.3
1000	900	844.4	783.2	840.6	560.2
1500	1100	994.0	873.8	990.8	298.0
1500	1300	1211.6	1115.1	1209.0	754.2
2000	1500	1361.2	1205.6	1358.9	503.8
2000	1800	1686.1	1563.1	1684.2	1115.3
2500	1800	1618.0	1411.9	1616.1	344.7
2500	2200	2053.8	1895.6	2052.2	1311.0
3000	2200	1985.7	1744.6	1984.1	586.4
3000	2600	2421.4	2227.9	2420.0	1504.6
3500	2500	2242.3	1950.2	2240.9	358.9
3500	3100	2896.2	2676.5	2895.1	1867.8
4000	2900	2610.2	2283.3	2608.9	643.3
4000	3500	3263.9	3008.9	3262.9	2062.5

Table 8

Branching ratios of the Z'_η boson into SM and BSM channels, varying $m_{Z'}$ and $m^0_{\tilde{\ell}}$, given in TeV, along the lines described in the text. $\mathrm{BR_{SM}}$ and $\mathrm{BR_{BSM}}$ denote the total branching fractions, respectively.

$m_{Z'}$	$m^0_{\tilde{\ell}}$	$\mathrm{BR}_{q\bar{q}}$	$\mathrm{BR}_{\ell^+\ell^-}$	$\mathrm{BR}_{\nu\bar{\nu}}$	$\mathrm{BR}_{W^+W^-}$	BR_{Zh}	$\mathrm{BR}_{\tilde{\chi}^+\tilde{\chi}^-}$	$\mathrm{BR}_{\tilde{\chi}^0\tilde{\chi}^0}$	$\mathrm{BR}_{\tilde{\nu}\tilde{\nu}*}$	$\mathrm{BR_{SM}}$	$\mathrm{BR_{BSM}}$
1.0	0.8	39.45	5.24	27.26	3.01	2.91	4.92	8.64	8.54	74.97	25.03
1.0	0.9	43.14	5.73	29.81	3.30	3.18	5.38	9.45	0.00	81.98	18.02
1.5	1.1	37.82	4.93	25.63	2.71	2.67	5.16	9.76	11.31	71.10	28.90
1.5	1.3	42.65	5.56	28.90	3.06	3.01	5.82	11.00	0.00	80.16	19.84
2.0	1.5	37.97	4.91	25.54	2.66	2.64	5.33	10.33	10.61	71.48	28.52
2.0	1.8	42.47	5.49	28.57	2.98	2.95	5.96	11.56	0.00	79.52	20.48
2.5	1.8	37.46	4.83	25.12	2.60	2.59	5.33	10.44	11.61	70.02	29.98
2.5	2.2	42.39	5.47	28.42	2.94	2.93	6.02	11.81	0.00	79.21	20.79
3.0	2.2	37.60	4.84	25.17	2.59	2.59	5.38	10.61	11.14	70.19	29.81
3.0	2.6	42.31	5.45	28.32	2.92	2.91	6.06	11.94	0.00	78.64	21.36
3.5	2.5	37.30	4.80	24.94	2.56	2.56	5.36	10.61	11.73	69.59	30.41
3.5	3.1	42.26	5.43	28.25	2.90	2.90	6.07	12.02	0.00	78.84	21.16
4.0	2.9	37.41	4.81	25.00	2.56	2.56	5.39	10.70	11.38	69.78	30.22
4.0	3.5	42.22	5.43	28.21	2.89	2.89	6.08	12.07	0.00	78.74	21.26

accessible, with branching ratios about 5–6% (charginos) and 10–12% (neutralinos). Decays into W^+W^- pairs or Higgs bosons associated with Z's are also permitted, with rates about 3%. The decrease of the sneutrino rate for large $m^0_{\tilde{\ell}}$ results in an enhancement of the SM branching ratios into $q\bar{q}$ and neutrino pairs. As a whole, summing up the contributions from sneutrinos, charginos and neutralinos, the branching ratio into BSM particles runs from 24 to 33%, thus displaying the relevance of those decays in any analysis on Z' production in a supersymmetric scenario.

5.2. Reference Point: Z'_ψ

An extra group $\mathrm{U}(1)'$ with a mixing angle $\theta = 0$ leads to a neutral vector boson labelled as Z'_ψ (Table 1). In Table 9, we quote the slepton masses for a few values of $m_{Z'}$ and $m^0_{\tilde{\ell}}$: as before,
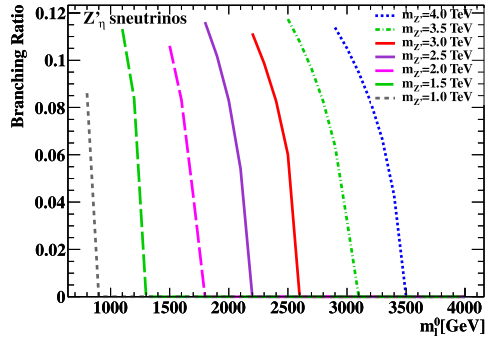
Fig. 16. Branching ratio of the Z'_η boson into sneutrino pairs $\tilde{\nu}_2\tilde{\nu}_2^*$, as a function of the slepton mass $m_{\tilde{\ell}}^0$, for several values of $m_{Z'}$.

Table 9
Slepton masses in GeV at the Reference Point for the model Z'_ψ and a few values of $m_{Z'}$ and $m_{\tilde{\ell}}^0$.

$m_{Z'}$	$m_{\tilde{\ell}}^0$	$m_{\tilde{\ell}_1}$	$m_{\tilde{\ell}_2}$	$m_{\tilde{\nu}_1}$	$m_{\tilde{\nu}_2}$
1000	400	535.2	194.2	529.2	189.2
1000	700	785.1	606.4	781.0	604.8
1500	600	801.7	285.4	797.7	282.0
1500	1000	1132.6	849.4	112.7	848.3
2000	800	1068.4	377.8	1065.4	375.2
2000	1300	1480.3	1092.1	1478.2	1091.2
2500	1000	1335.2	470.6	1333.8	468.6
2500	1600	1828.3	1334.7	1826.6	1334.0
3000	1100	1528.5	296.2	1526.4	292.9
3000	1900	2176.3	1577.2	2174.9	1576.6
3500	1300	1795.2	401.8	1793.4	399.4
3500	2200	2524.4	1819.7	2523.2	1819.2
4000	1500	2061.9	502.7	2060.4	500.8
4000	2500	2872.5	2062.2	2871.4	2061.7
4500	1600	2256.7	177.4	2255.3	171.9
4500	2800	3220.7	2304.7	3219.7	2304.2
5000	1800	2523.2	343.1	2521.9	340.3
5000	3100	3568.8	2547.1	3567.9	2546.7

the results are presented for the two values of $m_{\tilde{\ell}}^0$ which are found to enhance and minimize the slepton rate. For any mass value, the D-term enhances by few hundreds GeV the masses of $\tilde{\ell}_1$ and $\tilde{\nu}_1$ and strongly decreases $m_{\tilde{\ell}_2}$ and $m_{\tilde{\ell}_2}$, especially for small $m_{\tilde{\ell}}^0$ and large $m_{Z'}$. In Table 10 we present the branching ratios into all channels, for the same values of $m_{Z'}$ and $m_{\tilde{\ell}}^0$ as in Table 9. Unlike the Z'_η case, supersymmetric decays into charged-slepton pairs are allowed for $\theta = 0$, with a branching ratio, about 2%, roughly equal to the sneutrino rate. Furthermore, even the decays into gauginos are relevant, with rates into $\tilde{\chi}^+\tilde{\chi}^-$ and $\tilde{\chi}^0\tilde{\chi}^0$ about 10 and 20%, respectively. The decays into boson pairs, i.e. Zh and W^+W^-, are also non-negligible and account for about 3% of the total Z'_ψ width.

As a whole, the Z'_ψ modelling above depicted yields branching ratios of the order of 35–40% into BSM particle, and therefore it looks like being a promising scenario to investigate Z'

Table 10
Branching ratios of the Z'_ψ boson into SM and BSM channels, varying $m_{Z'}$ and m_ℓ^0. The masses are expressed in TeV.

$m_{Z'}$	m_ℓ^0	$\mathrm{BR}_{q\bar{q}}$	$\mathrm{BR}_{\ell^+\ell^-}$	$\mathrm{BR}_{\nu\bar{\nu}}$	$\mathrm{BR}_{W^+W^-}$	BR_{Zh}	$\mathrm{BR}_{\tilde{\chi}^+\tilde{\chi}^-}$	$\mathrm{BR}_{\tilde{\chi}^0\tilde{\chi}^0}$	$\mathrm{BR}_{\tilde{\nu}\tilde{\nu}*}$	$\mathrm{BR}_{\ell\tilde{\ell}*}$	$\mathrm{BR}_{\mathrm{SM}}$	$\mathrm{BR}_{\mathrm{BSM}}$
1.0	0.4	48.16	8.26	8.26	3.00	2.89	9.13	16.53	1.91	1.90	67.69	32.31
1.0	0.7	50.07	8.59	8.59	3.08	2.99	9.49	17.18	0.00	0.00	70.33	29.67
1.5	0.6	46.78	7.90	7.90	2.71	2.69	9.73	18.64	1.83	1.83	65.28	34.72
1.5	1.0	48.55	8.20	8.20	2.81	2.79	10.10	19.35	0.00	0.00	67.76	32.24
2.0	0.8	46.30	7.77	7.77	2.62	2.62	9.92	19.37	1.80	1.80	64.47	35.53
2.0	1.3	48.03	8.06	8.06	2.72	2.72	10.29	20.10	0.00	0.00	66.88	33.12
2.5	1.0	46.01	7.70	7.70	2.58	2.59	9.99	19.68	1.79	1.78	64.00	36.00
2.5	1.6	47.72	7.99	7.99	2.67	2.68	10.36	20.41	0.00	0.00	66.37	33.63
3.0	1.1	45.35	7.58	7.58	2.53	2.54	9.92	19.63	1.86	1.86	63.04	36.96
3.0	1.9	47.10	7.88	7.88	2.62	2.64	10.30	20.39	0.00	0.00	65.47	34.53
3.5	1.3	44.91	7.50	7.50	2.49	2.51	9.86	19.58	1.83	1.83	62.41	37.59
3.5	2.2	46.61	7.79	7.79	2.59	2.61	10.24	20.32	0.00	0.00	64.78	35.22
4.0	1.5	44.60	7.45	7.45	2.47	2.49	9.82	19.53	1.80	1.80	61.96	38.04
4.0	2.5	46.26	7.72	7.72	2.56	2.58	10.19	20.26	0.00	0.00	64.27	35.73
4.5	1.6	44.32	7.40	7.40	2.45	2.47	9.78	19.47	1.84	1.84	61.56	38.44
4.5	2.8	46.01	7.68	7.68	2.54	2.57	10.15	20.21	0.00	0.00	63.91	36.09
5.0	1.8	44.16	7.37	7.37	2.44	2.46	9.76	19.44	1.82	1.82	61.33	38.67
5.0	3.1	45.83	7.65	7.65	2.53	2.55	10.13	20.18	0.00	0.00	63.65	36.35
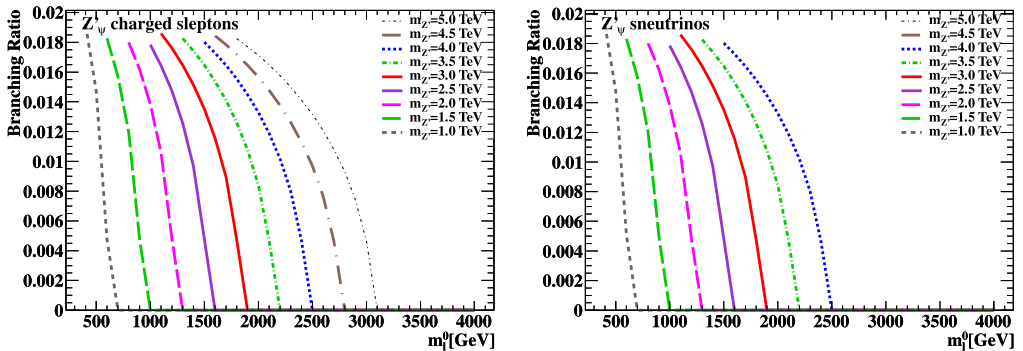
Fig. 17. Dependence of the Z'_ψ branching ratio into charged sleptons (left) and sneutrinos (right) as a function of m_ℓ^0, for several values of $m_{Z'}$.

production within the MSSM. Fig. 17 finally displays the branching ratios into sneutrinos and charged sleptons as a function of m_ℓ^0 and for several values of $m_{Z'}$.

5.3. Reference Point: Z'_N

In this subsection we investigate the phenomenology of the Z'_N boson, i.e. a U(1)$'$ gauge group with a mixing angle $\theta = \arctan\sqrt{15} - \pi/2$ (Table 1), along the lines of the previous sections. As discussed above, the Z'_N model is interesting since it corresponds to the Z'_χ model, but with the unconventional assignment of the SO(10) representations. Referring to the notation in Eq. (5), in the unconventional E$_6$ model the fields H and D^c are in the representation **16** and L and d^c in the **10** of SO(10).

Table 11

Slepton masses in the Z'_N model, varying $m_{Z'}$ and $m^0_{\tilde{\ell}}$, as discussed in the text. All masses are given in GeV.

$m_{Z'}$	$m^0_{\tilde{\ell}}$	$m_{\tilde{\ell}_1}$	$m_{\tilde{\ell}_2}$	$m_{\tilde{\nu}_1}$	$m_{\tilde{\nu}_2}$
1000	400	601.1	249.7	595.8	400.0
1000	600	749.2	512.2	745.0	600.0
1500	500	837.4	165.4	833.6	500.0
1500	900	1123.1	766.4	1120.2	900.0
2000	700	1136.4	303.9	1133.6	700.0
2000	1200	1497.1	1021.0	1495.0	1200.0
2500	800	1375.8	131.8	1372.9	800.0
2500	1500	1871.2	1275.7	1869.5	1500.0
3000	1000	1673.7	319.9	1671.8	1000.0
3000	1800	2245.3	1530.4	2243.9	1800.0
3500	1200	1972.6	466.2	1971.0	1200.0
3500	2100	2619.4	1785.3	2618.2	2100.0
4000	1300	2211.6	303.9	2210.2	1300.0
4000	2400	2993.6	2040.2	2992.5	2400.0
4500	1500	2510.2	476.8	2509.0	1500.0
4500	2700	3367.7	2295.1	3366.7	2700.0
5000	1600	2749.8	249.7	2748.6	1600.0
5000	3100	3822.5	2666.9	3821.6	3100.0

Table 11 presents the slepton masses varying $m_{Z'}$ and for the values of $m^0_{\tilde{\ell}}$ which minimize and maximize the slepton rate. The D-term addition to $m^0_{\tilde{\ell}}$ increases the mass of $\tilde{\ell}_1$ and $\tilde{\nu}_1$ and decreases the mass of $\tilde{\ell}_2$; its impact on $\tilde{\nu}_2$ is negligible and one can assume $m_{\tilde{\nu}_2} \simeq m^0_{\tilde{\ell}}$. Both decays into $\tilde{\ell}_2^+ \tilde{\ell}_2^-$ and $\tilde{\nu}_2 \tilde{\nu}_2^*$ are kinematically allowed, whereas $\tilde{\ell}_1$ and $\tilde{\nu}_1$ are too heavy to contribute to the Z' width.

Table 12 quotes the branching ratios for the Z'_N, computed for the same values of $m_{Z'}$ and $m^0_{\tilde{\ell}}$ as in Table 11. Although $Z'_N \to \tilde{\nu}_2 \tilde{\nu}_2^*$ is kinematically allowed, the coupling of the Z'_N to sneutrinos is zero for $\theta = \arctan \sqrt{15} - \pi/2$, since, as will be discussed in Appendix A, the rate into right-handed sfermions vanishes for equal vector and vector-axial coupling, i.e. $v_{\tilde{\nu}} = a_{\tilde{\nu}}$: therefore, this decay mode can be discarded. As for the other supersymmetric channels, the rates into charginos and neutralinos are quite significant and amount to about 9% and 28%, respectively. The decays into W^+W^- and Zh states account for approximately 1–2%, whereas the branching ratio into charged-slepton pairs is about 1%, even in the most favourable case. As a whole, the rates into BSM final states run from 18 to about 35% and therefore are a relevant contribution to the total Z' cross section. Fig. 18 finally presents the variation of the charged-slepton branching ratio as a function of $m^0_{\tilde{\ell}}$, for a few values of $m_{Z'}$.

5.4. Reference Point: Z'_I

The U(1)'-based model leading to a Z'_I, i.e. a mixing angle $\theta = \arccos \sqrt{5/8} - \pi/2$, has been extensively discussed, as it corresponds to the Representative Point. It exhibits the property that the initial slepton mass $m^0_{\tilde{\ell}}$ can be as low as a few GeV, still preserving a physical scenario for the sfermion masses. In the following, we shall assume a lower limit of $m^0_{\tilde{\ell}} = 200$ GeV and present results also for 1 TeV, in order to give an estimate of the dependence on $m^0_{\tilde{\ell}}$.

In Table 13 the charged- and neutral-slepton masses are listed for a few values of $m_{Z'}$ and $m^0_{\tilde{\ell}}$. We already noticed, when discussing the Representative Point and Fig. 3, that the D-term correc-

Table 12
Branching ratios of the Z'_N boson in SM and BSM channels, varying $m_{Z'}$ and $m^0_{\tilde{\ell}}$. Slepton and Z' masses are quoted in TeV.

$m_{Z'}$	$m^0_{\tilde{\ell}}$	$BR_{q\bar{q}}$	$BR_{\ell^+\ell^-}$	$BR_{\nu\bar{\nu}}$	$BR_{W^+W^-}$	BR_{Zh}	$BR_{\tilde{\chi}^+\tilde{\chi}^-}$	$BR_{\tilde{\chi}^0\tilde{\chi}^0}$	$BR_{\tilde{\ell}^+\tilde{\ell}^-}$	BR_{SM}	BR_{BSM}
1.0	0.4	49.51	11.98	9.59	1.71	1.68	8.71	15.78	1.04	72.79	27.21
1.0	0.6	50.03	12.11	9.69	1.73	1.69	8.80	15.94	0.00	73.56	26.44
1.5	0.5	47.99	11.51	9.21	1.57	1.57	9.26	17.76	1.12	70.28	29.72
1.5	0.9	48.53	11.64	9.31	1.59	1.59	9.36	17.96	0.00	71.08	28.92
2.0	0.7	47.50	11.36	9.08	1.53	1.54	9.44	18.46	1.08	69.47	30.53
2.0	1.2	48.02	11.48	9.18	1.54	1.55	9.55	18.66	0.00	70.22	29.78
2.5	0.8	47.16	11.26	9.01	1.50	1.52	9.50	18.73	1.12	68.92	31.08
2.5	1.5	47.69	11.38	9.11	1.52	1.53	9.61	18.94	0.00	69.70	30.30
3.0	1.0	46.43	11.30	8.86	1.47	1.49	9.43	18.66	1.08	67.83	32.17
3.0	1.8	46.94	11.20	8.96	1.49	1.50	9.53	18.86	0.00	68.58	31.42
3.5	1.2	45.85	10.93	8.74	1.45	1.47	9.35	18.56	1.05	66.98	33.02
3.5	2.1	46.34	11.05	8.84	1.46	1.48	9.45	18.76	0.00	67.68	32.32
4.0	1.3	45.42	10.83	8.66	1.43	1.45	9.29	18.47	1.07	66.34	33.66
4.0	2.4	45.91	10.94	8.75	1.45	1.47	9.39	18.67	0.00	67.06	32.94
4.5	1.5	45.13	10.75	8.60	1.42	1.44	9.24	18.41	1.05	65.90	34.10
4.5	2.7	45.60	10.87	8.70	1.44	1.46	9.34	18.60	0.00	66.61	33.39
5.0	1.6	44.90	10.70	8.56	1.41	1.43	9.21	18.35	1.06	65.56	34.44
5.0	3.1	45.38	10.81	8.65	1.43	1.45	9.31	18.55	0.00	66.27	33.73
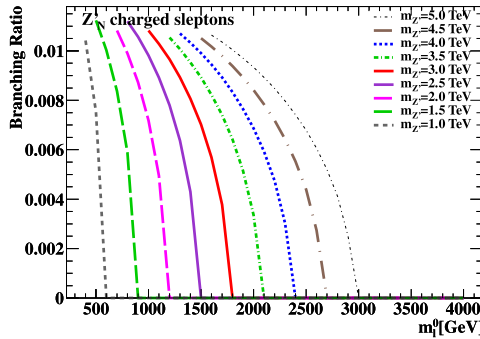
Fig. 18. Slepton branching ratios of the Z'_N boson as a function of $m^0_{\tilde{\ell}}$.

tion to the slepton mass is quite important for $\tilde{\ell}_1$, $\tilde{\nu}_1$ and $\tilde{\nu}_2$, especially for small values of $m^0_{\tilde{\ell}}$: this behaviour is confirmed by Table 13. The D-term turns out to be positive and quite large and the only kinematically permitted decay into sfermions is $Z'_I \rightarrow \tilde{\ell}_2\tilde{\ell}^*_2$. However, as in the Z'_N case, the vector and vector-axial coupling are equal, i.e. $v_{\tilde{\ell}} = a_{\tilde{\ell}}$, thus preventing this decay mode for the reasons which will be clarified in Appendix A. The conclusion is that in the Reference Point scenario, the Z'_I boson can decay into neither charged nor neutral sleptons. Therefore, the dependence of the branching ratios on $m^0_{\tilde{\ell}}$ is not interesting and Table 14 just reports the decay rates for fixed $m^0_{\tilde{\ell}} = 1$ TeV. The total BSM branching ratio lies between 12 and 17% and is mostly due to decays into chargino ($\sim 4\%$) and neutralino (~ 8–9%) pairs. Decays involving supersymmetric Higgs bosons, such as H^+H^-, $W^\pm H^\mp$ and HA final states, are possible, but with a total branching ratio which is negligible for small Z' masses and at most 3% for $m_{Z'} > 4$ TeV. As for the decay into SM quarks, it was already pointed out in Table 6 that the rate into $u\bar{u}$ pairs is

Table 13

Slepton masses in the U(1)$'$ scenario corresponding to a Z'_I boson, for a few values of $m_{Z'}$ and $m^0_{\tilde{\ell}}$. All masses are expressed in GeV.

$m_{Z'}$	$m^0_{\tilde{\ell}}$	$m_{\tilde{\ell}_1}$	$m_{\tilde{\ell}_2}$	$m_{\tilde{\nu}_1}$	$m_{\tilde{\nu}_2}$
1000	200	736.3	204.7	732.0	734.8
1000	1000	1226.6	1001.0	1223.0	1224.7
1500	200	1080.4	204.7	1077.4	1079.3
1500	1000	1458.5	1001.0	1456.3	1457.7
2000	200	1429.1	204.7	1426.8	1428.3
2000	1000	1732.7	1001.0	1730.8	1732.0
2500	200	1779.7	204.7	1777.9	1779.0
2500	3000	3482.4	3000.3	3481.5	3482.1
3000	200	2131.5	204.7	2129.7	2130.7
3000	3000	3674.5	3000.3	3673.7	3674.2
3500	200	2483.4	204.7	2482.1	2482.9
3500	3000	3889.4	3000.3	3888.5	3889.1
4000	200	2836.9	204.7	2834.8	2835.5
4000	3000	4123.4	3000.3	4122.6	4123.1
4500	200	3188.6	204.7	3187.6	3188.3
4500	3000	4373.5	3000.3	4372.7	4373.2
5000	200	3541.5	204.7	3540.6	3541.2
5000	3000	4637.0	3000.3	4636.4	4636.8

Table 14

Branching ratios of the Z'_I into SM and BSM particles for $m^0_{\tilde{\ell}} = 1$ TeV and varying $m_{Z'}$. The Z' mass is expressed in TeV.

$m_{Z'}$	$m^0_{\tilde{\ell}}$	$BR_{q\bar{q}}$	$BR_{\ell^+\ell^-}$	$BR_{\nu\bar{\nu}}$	$BR_{H^+H^-}$	$BR_{H^\pm}$	BR_{HA}	$BR_{\tilde{\chi}^+\tilde{\chi}^-}$	$BR_{\tilde{\chi}^0\tilde{\chi}^0}$	BR_{SM}	BR_{BSM}
1.0	1.0	44.06	14.69	29.37	0.00	$\mathcal{O}(10^{-3})$	$\mathcal{O}(10^{-4})$	4.31	7.58	88.11	11.89
1.5	1.0	43.39	14.46	28.93	0.00	$\mathcal{O}(10^{-4})$	$\mathcal{O}(10^{-4})$	4.56	8.65	86.78	13.22
2.0	1.0	43.16	14.38	28.77	0.00	$\mathcal{O}(10^{-4})$	$\mathcal{O}(10^{-3})$	4.65	9.03	86.31	13.69
2.5	1.0	42.99	14.33	28.66	0.06	$\mathcal{O}(10^{-3})$	0.07	4.68	9.19	85.98	14.02
3.0	1.0	42.53	14.18	28.36	0.53	$\mathcal{O}(10^{-3})$	0.53	4.66	9.20	85.07	14.93
3.5	1.0	42.16	14.05	28.11	0.91	$\mathcal{O}(10^{-3})$	0.92	4.64	9.19	84.33	15.67
4.0	1.0	41.90	13.96	27.93	1.20	$\mathcal{O}(10^{-3})$	1.21	4.62	9.17	83.79	16.21
4.5	1.0	41.70	13.90	27.80	1.40	$\mathcal{O}(10^{-3})$	1.41	4.61	9.16	83.40	16.60
5.0	1.0	41.56	13.85	27.71	1.56	0.01	1.57	4.60	9.15	83.12	16.88

zero since the couplings v_u and a_u (see also Appendix A) vanish for $\theta = \arccos\sqrt{5/8} - \pi/2$. Therefore, in Table 14, $BR_{q\bar{q}}$ only accounts for decays into down quarks.

5.5. Reference Point: Z'_S

The Z'_S boson corresponds to a mixing angle $\theta = \arctan(\sqrt{15}/9) - \pi/2$. As in the Z'_I model, one can set a small value of the initial slepton mass, such as $m^0_{\tilde{\ell}} = 200$ GeV, and still have a meaningful supersymmetric spectrum. The results on slepton masses and branching ratios are

Table 15
Slepton masses at the Reference Point with a Z'_S gauge boson and for few values of $m_{Z'}$ and $m_{\tilde{\ell}}^0$, given in GeV, as debated in the text.

$m_{Z'}$	$m_{\tilde{\ell}}^0$	$m_{\tilde{\ell}_1}$	$m_{\tilde{\ell}_2}$	$m_{\tilde{\nu}_1}$	$m_{\tilde{\nu}_2}$
1000	200	917.9	376.8	914.4	1020.0
1000	1000	1342.6	1049.7	1340.2	1414.3
1500	200	1357.4	516.7	1355.0	1513.4
1500	1000	1674.1	1107.7	1672.2	1802.9
2000	200	1800.7	664.8	1798.9	2010.0
2000	1000	2050.0	1184.0	2048.4	2236.1
2500	200	2245.5	816.7	2244.1	2508.0
2500	3000	3742.0	3102.7	3741.1	3905.2
3000	200	2691.2	970.5	2690.0	3006.7
3000	3000	4025.2	3146.7	4024.4	4242.7
3500	200	3137.3	1125.6	3136.3	3505.7
3500	3000	4336.2	3198.0	4335.4	4609.8
4000	200	3583.6	1281.4	3582.7	4005.0
4000	3000	4669.3	3256.1	4668.6	5000.0
4500	200	4030.2	1437.7	4029.4	4504.5
4500	3000	5020.2	3320.7	5019.6	5408.4
5000	200	4476.9	1594.3	4476.2	5004.0
5000	3000	5385.4	3391.4	5384.8	5831.0

summarized in Tables 15 and 16. Since the Z'_S decay rates are roughly independent of the slepton mass, in Table 16 the branching ratios are quoted only for $m_{\tilde{\ell}}^0 = 200$ GeV. From Table 15 we learn that the D-term contribution to slepton masses is positive and that $Z'_S \to \tilde{\ell}_2 \tilde{\ell}_2^*$ is the only decay kinematically allowed, at least for relatively small values of $m_{\tilde{\ell}}^0$. However, as displayed in Table 15, the branching ratio into such charged sleptons is very small, about 0.1%, even for low $m_{\tilde{\ell}}^0$ values. As for the other BSM decay modes, the most relevant ones are into chargino (about 3%) and neutralino (about 6–7%) pairs, the others being quite negligible. It is interesting, however, noticing that for $m_{Z'} = 5$ TeV the branching ratio into squark pairs starts to play a role, amounting to roughly 8%. In fact, although we set a high value like $m_{\tilde{q}}^0 = 5$ TeV, for relatively large Z' masses, i.e. $m_{Z'} > 3.8$ TeV, the D-term for $\tilde{d}_2$-type squarks starts to be negative, in such a way that $\tilde{d}_2 \tilde{d}_2^*$ final states are kinematically permitted. As a whole, one can say that, at the Reference Point, for $m_{Z'} < 5$ TeV the BSM decay rate is about 10–12%, but it becomes much higher for larger Z' masses, even above 20%, due to the opening of the decay into squark pairs. However, since the experimental signature of squark production is given by jets in the final state, it is quite difficult separating them from the QCD backgrounds. This scenario seems therefore not very promising for a possible discovery of supersymmetry via Z' decays.

5.6. Reference Point: Z'_χ

The U(1)$'$ group corresponding to a mixing angle $\theta = -\pi/2$ and a boson Z'_χ does not lead to a meaningful sfermion scenario in the explored range of parameters, as the sfermion masses

Table 16

Branching ratios of the Z'_S with the MSSM parameters at the Reference Point and for a few values of $m_{Z'}$, expressed in TeV. The initial slepton mass is fixed to 0.2 TeV, since the decay rates are independent of $m^0_{\tilde{\ell}}$.

$m_{Z'}$	$m^0_{\tilde{\ell}}$	$BR_{q\bar{q}}$	$BR_{\ell^+\ell^-}$	$BR_{\nu\bar{\nu}}$	$BR_{W^+W^-}$	BR_{Zh}	$BR_{\tilde{\chi}^+\tilde{\chi}^-}$	$BR_{\tilde{\chi}^0\tilde{\chi}^0}$	$BR_{\tilde{\ell}^+\tilde{\ell}^-}$	$BR_{\tilde{q}\tilde{q}*}$	BR_{SM}	BR_{BSM}
1.0	0.2	42.29	13.70	34.57	0.15	0.14	3.33	5.75	0.07	0.00	90.71	9.29
1.5	0.2	41.84	13.54	34.16	0.15	0.14	3.51	6.59	0.07	0.00	89.68	10.32
2.0	0.2	41.67	13.48	34.02	0.14	0.14	3.57	6.90	0.08	0.00	89.32	10.68
2.5	0.2	41.56	13.44	33.91	0.14	0.14	3.59	7.03	0.08	0.00	89.06	10.94
3.0	0.2	41.25	13.34	33.66	0.14	0.14	3.58	7.06	0.08	0.00	88.39	11.61
3.5	0.2	40.99	13.26	33.45	0.14	0.14	3.57	7.07	0.08	0.00	87.84	12.16
4.0	0.2	40.81	13.20	33.30	0.14	0.14	3.56	7.07	0.08	0.00	87.44	12.56
4.5	0.2	40.67	13.15	33.19	0.14	0.14	3.56	7.07	0.08	0.00	87.15	12.85
5.0	0.2	37.34	12.07	30.46	0.13	0.13	3.27	6.50	0.07	7.97	80.00	20.00

Table 17

Branching ratios of the Z'_χ boson as a function of the Z' mass, given in TeV. The rates into sfermion pairs are not presented, since the sfermion mass spectrum is unphysical for the Z'_χ model in the Reference Point scenario.

$m_{Z'}$	$BR_{q\bar{q}}$	$BR_{\ell^+\ell^-}$	$BR_{\nu\bar{\nu}}$	$BR_{W^+W^-}$	$BR_{H^+H^-}$	BR_{ZH}	BR_{hA}	BR_{SM}	BR_{BSM}
1.0	44.35	12.44	42.29	0.90	0.00	0.02	$\mathcal{O}(10^{-3})$	99.98	0.02
2.0	44.32	12.34	41.96	0.84	0.00	0.28	0.26	99.46	0.54
3.0	44.03	12.24	41.63	0.82	0.24	0.53	0.52	98.71	1.29
4.0	43.84	12.18	41.43	0.82	0.46	0.64	0.63	98.27	1.73
5.0	43.74	12.15	41.33	0.81	0.58	0.70	0.69	98.03	1.97

are unphysical after the addition of the D-term. This feature of the Z'_χ model, already observed in the Representative Point parametrization (see Section 4.1 and the $m_{\tilde{d}_2}$ spectrum in Fig. 1), holds even for a higher initial squark mass, such as $m^0_{\tilde{q}} = 5$ TeV, as in the Reference Point. It is nevertheless worthwhile presenting in Table 17 the Standard Model branching ratios, along with those into Higgs and vector bosons in a generic Two Higgs Doublet Model. For any $m_{Z'}$ the rates into quark and neutrino pairs are the dominant ones, being about 40–45%, whereas the branching ratio into lepton states is approximately 12% and the other modes (W^+W^-, Zh, HA and H^+H^-) account for the remaining 1–3%.

5.7. Reference Point: Z'_{SSM}

A widely used model in the analyses of the experimental data is the Sequential Standard Model (SSM): in this framework the Z' coupling to SM and MSSM particles is the same as the Z boson. The SSM is considered as a benchmark, since the production cross section is only function of the Z' mass and there is no dependence on the mixing angle θ and possible new physics parameters, such as the MSSM ones.

As for the supersymmetric sector, the sfermion masses get the D-term contribution associated with the hyperfine splitting, Eq. (25), but not the one due to further extensions of the MSSM, namely Eq. (26), proportional to g'^2 in the case of U(1)'. Moreover, the Z'_{SSM} coupling to sfermions is simply given by $g_{SSM} = g_2/(2\cos\theta_W)$, as in the SM. Since the hyperfine-splitting D-term is quite small, the sfermion spectrum is physical even for low values of $m^0_{\tilde{\ell}}$. Table 18 reports the sfermion masses obtained at the Reference Point, Eq. (33), for a few values of $m_{Z'}$ and varying $m^0_{\tilde{\ell}}$ from 100 GeV to $m_{Z'}/2$, the highest value kinematically allowed. For $m^0_{\tilde{\ell}} = 100$ GeV, because of the D-term, $m_{\tilde{\nu}_1}$ decreases by about 25%, $m_{\tilde{\ell}_1}$ and $m_{\tilde{\ell}_2}$ slightly

Table 18
Slepton masses in the Z'_{SSM} model varying $m_{Z'}$ and $m_{\tilde{\ell}}^0$. All masses are quoted in GeV.

$m_{Z'}$	$m_{\tilde{\ell}}^0$	$m_{\tilde{\ell}_1}$	$m_{\tilde{\ell}_2}$	$m_{\tilde{\nu}_1}$	$m_{\tilde{\nu}_2}$
1000	100	110.6	109.1	76.6	100.0
1000	500	502.2	501.9	495.8	500
1500	100	110.6	109.1	76.6	100.0
1500	750	751.5	751.3	747.2	750.0
2000	100	110.6	109.1	76.6	100.0
2000	1000	1001.1	1000.9	997.9	1000.0
2500	100	110.6	109.1	76.6	100.0
2500	1250	1250.9	1250.8	1248.3	1250.0
3000	100	110.6	109.1	76.6	100.0
3000	1500	1001.1	1000.9	997.9	1000.0
3500	100	110.6	109.1	76.6	100.0
3500	1750	1750.6	1750.6	1748.8	1750.0
4000	100	110.6	109.1	76.6	100.0
4000	2000	2000.6	2000.5	1999.0	2000.0
4500	100	110.6	109.1	76.6	100.0
4500	2250	2250.5	2250.4	2249.1	2250.0
5000	100	110.6	109.1	76.6	100.0
5000	2500	2500.4	2500.4	2499.2	2500.0

increase and $m_{\tilde{\nu}_2}$ is roughly unchanged. For large values of $m_{\tilde{\ell}}^0$, the D-term is negligible and all slepton masses are approximately equal to $m_{\tilde{\ell}}^0$.

Tables 19 and 20 present, respectively, the SM and BSM branching ratios of the Z'_{SSM} at the Reference Point, for the values of Z' and slepton masses listed in Table 18. The decays into BSM particles exhibit rates, about 60–65%, which can be even higher than the SM ones, accounting for the remaining 35–40%. In fact, this turns out to be mostly due to the decays into neutralinos, accounting for more than 30%, and into charginos, about 16–18%. The branching fractions into sleptons are quite small: the one into sneutrinos is less than 4% and the one into charges sleptons about 1–2%. The W^+W^- mode contributes with a rate about 4–5%, the H^+H^- one is relevant only for $m_{Z'} > 2.5$ TeV, with a branching ratio which can reach 3%, the Zh and hA channels are accessible for $m_{Z'} > 1.5$ TeV, with decay fractions between 1 and 4%. The variation of the sneutrino and charged-slepton branching ratios as a function of the slepton mass at the Z' scale is displayed in Fig. 19 for 1 TeV $< m_{Z'} < 4$ TeV.

6. Cross sections and event rates at the LHC

In this section we present the total cross section for Z' production at the LHC according to the models discussed throughout this paper, i.e. Table 1, as well as the Sequential Standard Model. We consider pp collisions at three centre-of-mass energies: 7 TeV (the 2011 LHC run), 8 TeV (the 2012 run) and 14 TeV, the ultimate project energy. For each energy we shall calculate the cross section and estimate the expected number of events with a Z' boson decaying into supersymmetric particles, for a few values of integrated luminosity.

6.1. Leading order Z' production cross section

The cross sections are computed at leading order (LO), employing the LO parton distribution functions CTEQ6L [41] and setting the factorization scale equal to the Z' mass. Using a different

Table 19

Branching ratios into SM particles of the Z'_{SSM}, varying $m_{Z'}$ and $m_{\tilde{\ell}}^0$, as debated in the text. Slepton and Z' masses are expressed in TeV.

$m_{Z'}$	$m_{\tilde{\ell}}^0$	$BR_{q\bar{q}}$	$BR_{\ell^+\ell^-}$	$BR_{\nu\bar{\nu}}$	$BR_{W^+W^-}$	BR_{SM}
1.0	0.10	29.61	3.87	7.69	5.56	46.73
1.0	0.50	31.38	4.10	8.15	5.90	49.53
1.5	0.10	27.38	3.53	7.02	4.86	42.79
1.5	0.75	28.89	3.73	7.41	5.13	45.15
2.0	0.10	26.21	3.36	6.69	4.56	40.83
2.0	1.00	27.59	3.54	7.04	4.80	42.98
2.5	0.10	25.35	3.25	6.46	4.37	39.42
2.5	1.25	26.64	3.41	6.79	4.59	41.42
3.0	0.10	24.78	3.17	6.31	4.25	38.51
3.0	1.50	26.01	1.66	6.62	4.46	40.42
3.5	0.10	24.42	3.12	6.21	4.17	37.92
3.5	1.75	25.61	1.40	6.51	4.37	39.78
4.0	0.10	24.18	3.09	6.15	4.12	37.54
4.0	2.00	25.35	1.21	6.44	4.32	39.35
4.5	0.10	24.01	3.07	6.10	4.09	37.27
4.5	2.25	25.16	1.07	6.39	4.28	39.06
5.0	0.10	23.89	3.05	6.07	4.06	37.07
5.0	2.50	25.03	0.96	6.36	4.25	38.84

Table 20

Branching ratios into BSM particles of the Z'_{SSM} for a few values of $m_{Z'}$ and $m_{\tilde{\ell}}^0$, expressed in TeV.

$m_{Z'}$	$m_{\tilde{\ell}}^0$	$BR_{H^+H^-}$	BR_{Zh}	B_{hA}	$BR_{\tilde{\chi}^+\tilde{\chi}^-}$	$BR_{\tilde{\chi}^0\tilde{\chi}^0}$	$BR_{\tilde{\ell}^+\tilde{\ell}^-}$	$BR_{\tilde{\nu}\tilde{\nu}^*}$	BR_{BSM}
1.0	0.10	0.00	$\sim 10^{-6}$	0.00	18.31	29.30	1.89	3.77	53.27
1.0	0.50	0.00	$\sim 10^{-6}$	0.00	19.41	31.06	0.00	0.00	50.47
1.5	0.10	0.00	0.87	0.76	17.84	32.52	1.75	3.48	57.21
1.5	0.75	0.00	0.92	0.80	18.82	34.31	0.00	0.00	54.55
2.0	0.10	0.00	1.93	1.85	17.37	33.01	1.67	3.33	59.17
2.0	1.00	0.00	2.04	1.95	18.28	34.75	0.00	0.00	57.02
2.5	0.10	0.91	2.59	2.53	16.93	32.78	1.62	3.22	60.58
2.5	1.25	0.95	2.72	2.66	17.79	34.45	0.00	0.00	58.57
3.0	0.10	1.72	2.98	2.94	16.62	32.51	1.58	3.15	61.49
3.0	1.50	1.81	3.13	3.08	17.44	34.12	0.00	0.00	59.58
3.5	0.10	2.27	3.23	3.20	16.42	32.30	1.56	3.10	62.08
3.5	1.75	2.38	3.38	3.35	17.22	33.88	0.00	0.00	60.22
4.0	0.10	2.65	3.39	3.37	16.28	32.16	1.54	3.07	62.46
4.0	2.00	2.78	3.56	3.53	17.07	33.71	0.00	0.00	60.65
4.5	0.10	2.91	3.51	3.49	16.19	32.06	1.53	3.05	62.73
4.5	2.25	3.05	3.67	3.65	16.96	33.59	0.00	0.00	60.94
5.0	0.10	3.11	3.59	3.57	16.12	31.98	1.52	3.03	62.93
5.0	2.50	3.26	3.76	3.74	16.89	33.51	0.00	0.00	61.16

LO PDF has a negligible impact on the results. The cross section for Drell–Yan like processes has been computed up to next-to-next-to leading order (NNLO) in QCD and, in principle, the calculations carried out in Refs. [42,43] can be easily extended to Z' production processes. However, since all Z' partial widths and branching ratios have been evaluated at LO, for the sake of consistency, we decided to stick to the lowest-level approximation.
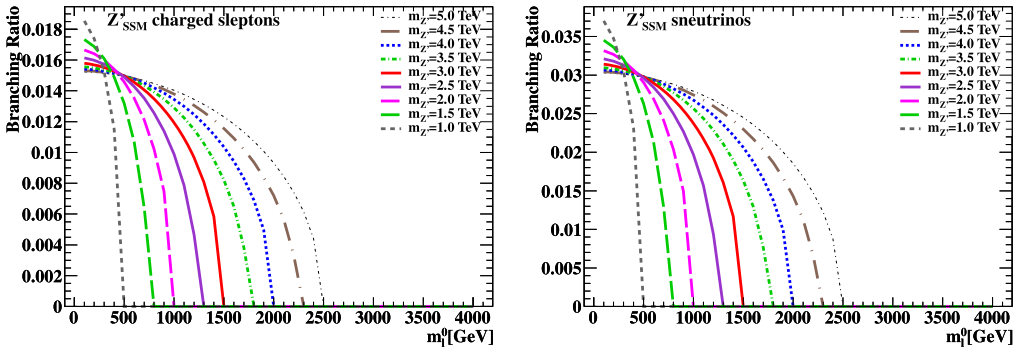
Fig. 19. Branching ratios of the Z'_{SSM} as a function of $m^0_{\tilde{\ell}}$ for several values of the Z' mass. Left: branching fraction into charged sleptons. Right: branching fraction into sneutrinos.

The parton-level process is analogous to Z production, i.e. it is the purely SM quark–antiquark annihilation $q\bar{q} \rightarrow Z'$. Since the coupling of the Z' to the quarks depends on the specific U(1)′ scenario, the production rate is a function of the mixing angle θ and of the Z' mass, but is independent of the MSSM parameters. In the Sequential Standard Model, the cross section just depends on the mass of the Z'_{SSM}. Figs. 20–22 present the total cross section for the different models investigated throughout this work, as a function of $m_{Z'}$, at the energies of 7 TeV (Fig. 20), 8 TeV (Fig. 21) and 14 TeV (Fig. 22). For each centre-of-mass energy, we present the results on linear (left) and logarithmic (right) scales. Tables 21, 22 and 23 quote the numerical values of the LO Z' production cross section, varying $m_{Z'}$ from 1 to 5 TeV, with steps of 500 GeV, in U(1)′ models and in the Sequential Standard Model.

The highest production cross section is given by the SSM, whereas the Z'_ψ model yields the lowest rate; the predictions of the other models lie between these results and are almost indistinguishable for large $m_{Z'}$. Moreover, the rates decrease by several orders of magnitude once $m_{Z'}$ increases. In detail, at $\sqrt{s} = 7$ TeV, the SSM cross section runs from 1.6 pb ($m_{Z'} = 1$ TeV) to $\mathcal{O}(10^{-8})$ pb ($m_{Z'} = 5$ TeV). The production rate for the U(1)′-based Z' varies from $\mathcal{O}(10^{-1})$ to $\mathcal{O}(10^{-9})$ pb in the same $m_{Z'}$ range, with very little differences among the models. At the centre-of-mass energy of 8 TeV, the variation is between 2.3 pb (Z'_{SSM} at $m_{Z'} = 1$ TeV) and $\mathcal{O}(10^{-9})$ pb (all other models at $m_{Z'} = 5$ TeV). At $\sqrt{s} = 14$ TeV, for a Z' mass of 1 TeV the cross section varies from about 8 pb (Z'_{SSM}) to 1.8 pb (Z'_ψ); for $m_{Z'} = 5$ TeV, all models yield a rate around $\mathcal{O}(10^{-4})$ pb.

6.2. Event rates with sparticle production in Z' decays at the LHC

In the following, we wish to investigate the domain where possible Z' decays into supersymmetric particles could be detectable. For this purpose, we consider two scenarios: $\sqrt{s} = 8$ TeV, with an integrated luminosity, $\int \mathcal{L} \, dt = 20 \text{ fb}^{-1}$, as expected in the 2012 LHC data taking, and, in future perspective, $\sqrt{s} = 14$ TeV with $\int \mathcal{L} \, dt = 100 \text{ fb}^{-1}$. In the narrow–width approximation, the foreseen number of events in Z' decays is simply given by the product of integrated luminosity, production cross section and relevant branching ratio.

The expected event rates in the two considered scenarios are summarized in Tables 24 and 25, for $m_{Z'} = 1.5$ and 2 TeV and setting the slepton mass $m^0_{\tilde{\ell}}$ to the values which in Tables 8–20 maximize the slepton rate. We discarded the Z'_χ model as it does not yield a sfermion spectrum
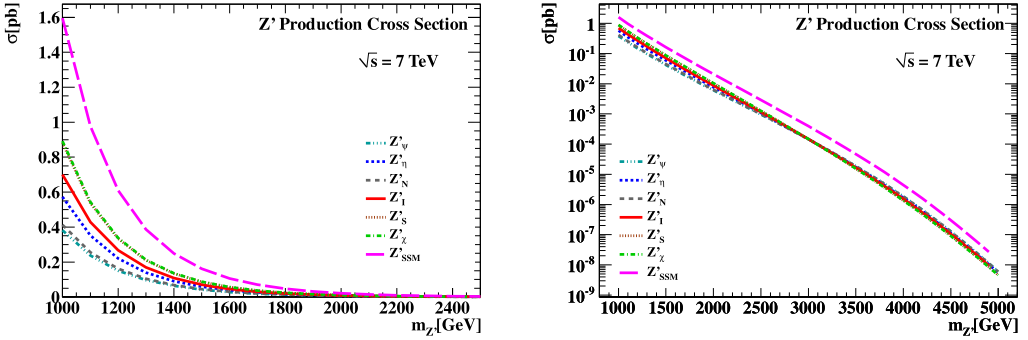
Fig. 20. Cross section of Z' production in pp collisions at 7 TeV. Left: linear scale. Right: logarithmic scale.
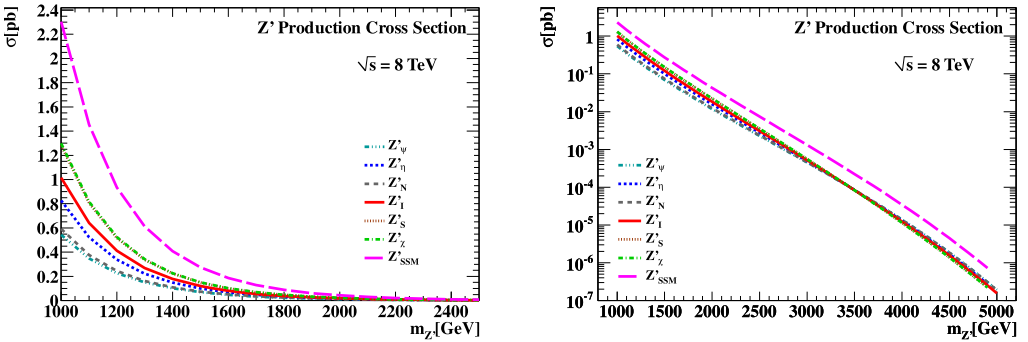

Fig. 21. Cross section for Z' production in pp collisions at 8 TeV. Left: linear scale. Right: logarithmic scale.
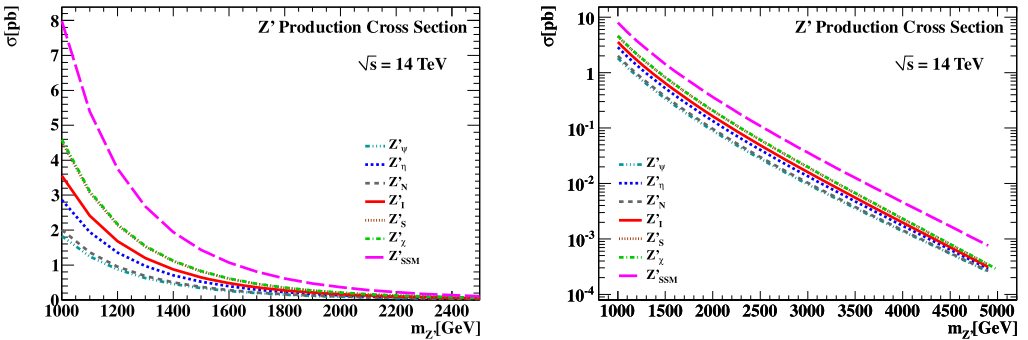
Fig. 22. Cross section for Z' production in pp collisions at 14 TeV. Left: linear scale. Right: logarithmic scale.

after the addition of the D-term to squark and slepton masses. As discussed in Section 5, leptonic final states in supersymmetric events can be yielded by direct decays $Z' \to \tilde{\ell}^+ \tilde{\ell}^-$ (Fig. 13) or by a cascade originated from primary decays into sneutrino, chargino or neutralino pairs (see Figs. 14 and 15). By adding up such rates, one obtains the so-called *cascade* branching ratio:

$$\mathrm{BR}_{\mathrm{casc}} = \mathrm{BR}_{\tilde{\nu}\tilde{\nu}^*} + \mathrm{BR}_{\tilde{\chi}^+\tilde{\chi}^-} + \mathrm{BR}_{\tilde{\chi}^0\tilde{\chi}^0}. \tag{34}$$

Table 21

LO Z' production cross section in pb at the LHC for pp collisions at $\sqrt{s} = 7$ TeV for the various models in Table 1 and $m_{Z'}$ varying from 1 to 5 TeV, with steps of 500 GeV. The CTEQ6L LO parton distribution functions are employed.

$m_{Z'}$	$\sigma(Z'_\eta)$	$\sigma(Z'_\psi)$	$\sigma(Z'_N)$	$\sigma(Z'_I)$	$\sigma(Z'_S)$	$\sigma(Z'_\chi)$	$\sigma(Z'_{SSM})$
1.0	0.57	0.38	0.41	0.70	0.88	0.89	1.59
1.5	6.3×10^{-2}	4.2×10^{-2}	4.5×10^{-2}	7.0×10^{-2}	8.6×10^{-2}	8.7×10^{-2}	0.16
2.0	7.7×10^{-3}	6.1×10^{-3}	6.4×10^{-3}	8.8×10^{-3}	1.0×10^{-2}	1.0×10^{-2}	2.1×10^{-2}
2.5	1.0×10^{-3}	9.6×10^{-4}	9.8×10^{-4}	1.2×10^{-3}	1.3×10^{-3}	1.3×10^{-3}	2.9×10^{-2}
3.0	1.5×10^{-4}	1.4×10^{-4}	1.4×10^{-4}	1.5×10^{-4}	1.5×10^{-4}	1.5×10^{-4}	3.9×10^{-4}
3.5	1.7×10^{-5}	1.9×10^{-5}	1.8×10^{-5}	1.7×10^{-5}	1.5×10^{-5}	1.5×10^{-5}	4.7×10^{-5}
4.0	1.7×10^{-6}	1.9×10^{-6}	1.8×10^{-6}	1.5×10^{-6}	1.4×10^{-6}	1.3×10^{-6}	4.4×10^{-6}
4.5	1.1×10^{-7}	1.3×10^{-7}	1.2×10^{-7}	1.0×10^{-7}	9.2×10^{-8}	9.1×10^{-8}	3.0×10^{-7}
5.0	5.5×10^{-9}	6.0×10^{-9}	5.9×10^{-9}	5.1×10^{-9}	4.6×10^{-9}	4.5×10^{-9}	1.4×10^{-8}

Table 22

As in Table 21, but at the centre-of-mass energy $\sqrt{s} = 8$ TeV.

$m_{Z'}$	$\sigma(Z'_\eta)$	$\sigma(Z'_\psi)$	$\sigma(Z'_N)$	$\sigma(Z'_I)$	$\sigma(Z'_S)$	$\sigma(Z'_\chi)$	$\sigma(Z'_{SSM})$
1.0	0.83	0.54	1.01	1.28	1.28	1.30	2.30
1.5	0.10	6.9×10^{-2}	7.4×10^{-2}	0.12	0.15	0.15	0.27
2.0	1.6×10^{-2}	1.2×10^{-2}	1.2×10^{-2}	1.8×10^{-2}	2.2×10^{-2}	2.2×10^{-2}	4.3×10^{-2}
2.5	2.8×10^{-3}	2.3×10^{-3}	2.4×10^{-3}	3.1×10^{-3}	3.5×10^{-3}	3.5×10^{-3}	7.4×10^{-3}
3.0	4.9×10^{-4}	4.5×10^{-4}	4.6×10^{-4}	5.2×10^{-4}	5.5×10^{-4}	5.6×10^{-4}	1.3×10^{-3}
3.5	8.4×10^{-5}	8.5×10^{-5}	8.5×10^{-5}	8.4×10^{-5}	8.3×10^{-5}	8.3×10^{-5}	2.2×10^{-4}
4.0	1.3×10^{-5}	1.4×10^{-5}	1.4×10^{-5}	1.2×10^{-5}	1.1×10^{-5}	1.1×10^{-5}	3.4×10^{-5}
4.5	1.7×10^{-6}	1.9×10^{-6}	1.8×10^{-6}	1.6×10^{-6}	1.4×10^{-6}	1.4×10^{-6}	4.4×10^{-6}
5.0	1.7×10^{-7}	1.9×10^{-7}	1.9×10^{-7}	1.6×10^{-7}	1.4×10^{-7}	1.4×10^{-7}	4.5×10^{-7}

Table 23

As in Tables 21 and 22, but at the centre-of-mass energy $\sqrt{s} = 14$ TeV.

$m_{Z'}$	$\sigma(Z'_\eta)$	$\sigma(Z'_\psi)$	$\sigma(Z'_N)$	$\sigma(Z'_I)$	$\sigma(Z'_S)$	$\sigma(Z'_\chi)$	$\sigma(Z'_{SSM})$
1.0	2.87	1.83	2.00	3.56	4.53	4.59	7.98
1.5	0.52	0.34	0.37	0.64	0.82	0.83	1.43
2.0	0.13	9.0×10^{-2}	9.7×10^{-2}	0.16	0.20	0.21	0.36
2.5	4.0×10^{-2}	2.8×10^{-2}	3.0×10^{-2}	4.9×10^{-2}	6.1×10^{-2}	6.2×10^{-2}	0.11
3.0	1.3×10^{-2}	9.7×10^{-3}	1.0×10^{-2}	1.6×10^{-2}	2.0×10^{-2}	2.0×10^{-2}	3.6×10^{-2}
3.5	4.8×10^{-3}	3.6×10^{-3}	3.8×10^{-3}	5.5×10^{-3}	6.6×10^{-3}	6.7×10^{-3}	1.3×10^{-2}
4.0	1.7×10^{-3}	1.4×10^{-3}	1.4×10^{-3}	2.0×10^{-3}	2.3×10^{-3}	2.3×10^{-3}	4.6×10^{-3}
4.5	6.4×10^{-4}	5.4×10^{-4}	5.6×10^{-4}	7.1×10^{-4}	8.0×10^{-4}	8.1×10^{-4}	1.7×10^{-3}
5.0	2.4×10^{-4}	2.1×10^{-4}	2.2×10^{-4}	2.5×10^{-4}	2.8×10^{-4}	2.8×10^{-4}	6.2×10^{-4}

In Tables 24 and 25 N_{slep} and N_{casc} are the number of events with a Z' decaying into a primary charged-slepton pairs or into a supersymmetric cascade, respectively. In both luminosity (energy) regimes, due to the large cross section, the Sequential Standard Model is the one yielding the highest production of supersymmetric particles in Z' decays, up to $\mathcal{O}(10^4)$–$\mathcal{O}(10^5)$ for cascade events at $\sqrt{s} = 14$ TeV and $\int \mathcal{L} \, dt = 100$ fb^{-1} and a Z' mass $m_{Z'} = 1.5$ TeV. As discussed in Sections 5.1 and 5.4, in the Z'_η and Z'_I models direct decays into charged sleptons are prevented, but sneutrino, neutralino and chargino productions are accessible, with expected number of events from 50 to $\mathcal{O}(10^4)$ according to $m_{Z'}$, energy and integrated luminosity. As for

Table 24
Number of supersymmetric particles at the LHC, for Z' production U(1)$'$ models and in the Sequential Standard Model at $\sqrt{s} = 8$ TeV and $\int \mathscr{L} \, dt = 20$ fb^{-1}, as a function of $m_{Z'}$ expressed in TeV.

Model	$m_{Z'}$	N_{casc}	N_{slep}
Z'_η	1.5	523	–
Z'_η	2	55	–
Z'_ψ	1.5	599	36
Z'_ψ	2	73	4
Z'_N	1.5	400	17
Z'_N	2	70	3
Z'_I	1.5	317	–
Z'_I	2	50	–
Z'_S	1.5	30	–
Z'_S	2	46	–
Z'_{SSM}	1.5	2968	95
Z'_{SSM}	2	462	14

Table 25
As in Table 24, but for $\sqrt{s} = 14$ TeV and $\int \mathscr{L} \, dt = 100$ fb^{-1}.

Model	$m_{Z'}$	N_{casc}	N_{slep}
Z'_η	1.5	13 650	–
Z'_η	2.0	2344	–
Z'_ψ	1.5	10 241	622
Z'_ψ	2.0	2784	162
Z'_N	1.5	9979	414
Z'_N	2.0	2705	104
Z'_I	1.5	8507	–
Z'_I	2.0	2230	–
Z'_S	1.5	8242	65
Z'_S	2.0	2146	16
Z'_{SSM}	1.5	775 715	24 774
Z'_{SSM}	2	19 570	606

the Z'_N model, in the high-luminosity phase, a few hundreds of direct sleptons and up to 10^4 cascade particles can be produced for $m_{Z'} = 1.5$ TeV. For $\int \mathscr{L} \, dt = 20$ fb^{-1} and $\sqrt{s} = 8$ TeV, direct slepton decays are negligible, but about 400 and 70 cascade events can be expected for a Z' mass of 1.5 and 2 TeV, respectively. The Z'_S boson leads to many cascade particles in the high-luminosity regime, between 10^3 and 10^4, and a few tenths of direct leptons. For the lower-luminosity case, there are no directly produced charged sleptons, whereas the cascade sparticles are about 30 ($m_{Z'} = 1.5$ TeV) and 46 ($m_{Z'} = 2$ TeV).

Before concluding this subsection, we point out that, although the numbers in Tables 24 and 25 encourage optimistic predictions on Z' decays into sparticles, especially in the high-luminosity phase, before drawing a conclusive statement on this issue, it will be necessary carrying out a careful study accounting for detector acceptance and resolution, triggering efficiency and cuts on final-state jets and leptons. Hence, the results presented in this paper should be seen a first step towards a more thorough investigation, which requires, above all, the implementation of the models herein discussed into a Monte Carlo event generator. In this perspective, one should compare the Monte Carlo predictions with the experimental data following, e.g., the approach

proposed in [44] or investigating the observables suggested in [45] to search for new physics in Drell–Yan like events mediated by a new heavy resonance. The same analysis should be also performed for the Standard Model backgrounds: as discussed in the Introduction, we shall defer the implementation of the modelling for Z' production and decays, as well as the comparison with the simulation of the backgrounds, to future work.

7. Conclusions

In this paper, we discussed production and decay of new neutral Z' bosons, according to new physics models based on a $U(1)'$ gauge group and in the Sequential Standard Model. Unlike most analyses undertaken so far, based on SM decays, we also included Z' supersymmetric decay modes, as predicted by the Minimal Supersymmetric Standard Model: in this perspective, the current Z' mass limits may have to be revisited. Extending the MSSM with the $U(1)'$ symmetry implies new features, such as an extra scalar neutral Higgs boson, two novel neutralinos and a modification of the sfermion masses due to an additional contribution to the so-called D-term. The particle mass spectra were studied in terms of the parameters characterizing the $U(1)'$ group and the MSSM; in particular, we discarded scenarios wherein, for fixed values of the sfermion soft mass, squarks or sleptons are not physical after the addition of the D-term. The same study has been performed for the purpose of the Z' partial widths and branching ratios, paying special attention to final states with charged leptons and missing energy. In fact, these configurations are favourable for an experimental detection at hadron colliders and can be yielded by intermediate charged sleptons or a supersymmetric cascade through neutralinos, chargino and sneutrinos. The branching ratios of these Z' decays have been investigated in all the models, as a function of the slepton mass.

We finally computed the Z' production LO cross section in all scenarios and gave an estimate of the number of supersymmetric events in Z' decays, in the narrow–width approximation and for few values of centre-of-mass energy and integrated luminosity. The outcome of this study is that, for some models and parametrizations, one can even have up to 10^4–10^5 events with sparticle production in Z' decays. As an additional remark, we wish to point out that the $Z' \to \tilde{\ell}^+ \tilde{\ell}^-$ decay presents two interesting features. First, the Z' mass will set an additional constrain on the slepton invariant mass; second, it allows the exploration of corners of the phase space which would be instead unaccessible through other processes, e.g. Drell–Yan like events.

In summary, we consider our investigation a useful starting point to study Z' production and decay beyond the Standard Model, such as within supersymmetric theories, drawing guidelines for future experimental analyses. In future perspective, it will be very interesting performing a study including parton showers, finite-width and hadronization corrections, as well as experimental effects, like the detector simulation and the acceptance cuts. In this way, one will eventually be able to draw a statement on the Z' mass limits within supersymmetry. To reach these objectives, the models for Z' production and decay, examined throughout this paper, will have to be implemented in Monte Carlo programs, such as HERWIG or PYTHIA, and the supersymmetry signals compared with the Standard Model backgrounds simulated, e.g., by means of the ALPGEN code [46]. In the framework of an event generator, it will also be possible, in the same manner as the experimental analyses do, rescaling the total cross section in such a way to include higher-order QCD corrections. For this purpose, the use of the FEWZ code [47], which simulates vector boson production at hadron colliders at NNLO, with fully exclusive final states, is planned. Other possible extensions of our analysis consist in investigating more thoroughly the unconventional assignment of the SM and exotic fields to the SU(10) representations, as well as scenarios wherein the exotic leptons (sleptons) and quarks (squarks), predicted by the grand-

unified group E_6, but discarded in the present work, are lighter than the Z' and therefore capable of contributing to its decay width. This is in progress.

Acknowledgements

Appendix A. Z' decay rates into standard and supersymmetric particles

The Lagrangian term describing the interaction of the Z' with fermions is given by:

$$\mathscr{L}_f = g' \bar{f} \gamma^\mu (v_f - a_f \gamma_5) f Z'_\mu, \tag{35}$$

with

$$f = \begin{pmatrix} f_L \\ f_R^c \end{pmatrix}. \tag{36}$$

Setting $Q'(f_R) = -Q'(f_L^c)$, the vector and axial-vector couplings read:

$$v_f = \frac{1}{2} \big[Q'(f_L) + Q'(f_R) \big], \qquad a_f = \frac{1}{2} \big[Q'(f_L) - Q'(f_R) \big], \tag{37}$$

where the U(1)$'$ charges of left- and right-handed fermions can be obtained by using Eq. (12) and Table 2. In terms of the mixing angle θ, such couplings read:

$$v_f = \frac{1}{2} \big[\big(Q'_\psi(f_L) + Q'_\psi(f_R) \big) \cos\theta - \big(Q'_\chi(f_L) + Q'_\chi(f_R) \big) \sin\theta \big],$$
$$a_f = \frac{1}{2} \big[\big(Q'_\psi(f_L) - Q'_\psi(f_R) \big) \cos\theta - \big(Q'_\chi(f_L) - Q'_\chi(f_R) \big) \sin\theta \big]. \tag{38}$$

One can thus write the Z' width into fermion pairs as:

$$\Gamma\big(Z' \to f\bar{f}\big) = C_f \frac{g'^2}{12\pi} m_{Z'} \left[v_f^2 \left(1 + 2\frac{m_f^2}{m_{Z'}^2} \right) + a_f^2 \left(1 - 4\frac{m_f^2}{m_{Z'}^2} \right) \right] \left(1 - 4\frac{m_f^2}{m_{Z'}^2} \right)^{1/2}, \tag{39}$$

where the colour factor is $C_f = 3$ for quarks and $C_f = 1$ for leptons. With the charges listed in Table 2 and employing Eq. (38), one can show that, in the Z'_I model, namely $\theta = \arccos\sqrt{5/8} - \pi/2$, the vector and vector-axial couplings of the Z' with up-type quarks vanish, i.e. $v_u = a_u = 0$. In fact, when discussing Z'_I phenomenology at the Representative Point (Section 4), it was pointed out that its branching ratio into $u\bar{u}$ pairs is null.

Likewise, the interaction Lagrangian of the sfermions with the Z' reads:

$$\mathscr{L}_{\tilde{f}} = g'(v_f \pm a_f) \big[\tilde{f}^*_{L,R} (\partial_\mu \tilde{f}_{L,R}) - (\partial_\mu \tilde{f}^*_{L,R}) \tilde{f}_{L,R} \big] Z'^\mu. \tag{40}$$

The width into left- or right-handed sfermions is given by:

$$\Gamma\big(Z' \to \tilde{f}_{L,R} \tilde{f}^*_{L,R}\big) = C_f \frac{g'^2}{48\pi} m_{Z'} (v_f \pm a_f)^2 \left(1 - 4\frac{m_{\tilde{f}}^2}{m_{Z'}^2} \right)^{1/2}, \tag{41}$$

where the $\pm$ sign refers to left- and right-handed sfermions, respectively. Eq. (41) is expressed in terms of weak eigenstates $\tilde{f}_{L,R}$; its generalization to the mass eigenstates $\tilde{f}_{1,2}$ is straightforward

and discussed in [12]. However, for the parametrizations used throughout this paper, sfermion mixing is always negligible and Eq. (41) can be safely used even to calculate the branching ratios into $\tilde{f}_1\tilde{f}_1^*$ and $\tilde{f}_2\tilde{f}_2^*$ final states.

From Eq. (41) one can learn that the Z' rate into left- and right-handed sfermions vanishes for $v_f = -a_f$ and $v_f = a_f$, respectively. In fact, for $v_f = a_f$, according to Eq. (35), the Z' only couples to left-handed fermions and therefore in the MSSM, in absence of left–right mixing, there is no coupling with right-handed sfermions. Likewise, for $v_f = -a_f$, the Z' only couples to right-handed fermions and sfermions and the rate into $\tilde{f}_L\tilde{f}_L^*$ pairs is null. For example, in the Z'_N model, it is $v_{\tilde{\nu}} = a_{\tilde{\nu}}$, whereas, in the Z'_I model, $v_{\tilde{\ell}} = a_{\tilde{\ell}}$. Therefore, as remarked in Sections 5.3 and 5.4, the $Z'_N \to \tilde{\nu}_2\tilde{\nu}_2^*$ and $Z'_I \to \tilde{\ell}_2\tilde{\ell}_2$ are suppressed, although they are kinematically permitted at the Reference Point.

As for the Higgs sector, defining Q'_1, Q'_2 and Q'_3 the U(1)$'$ charges as in Eq. (15) and $\beta = \arctan(v_2/v_1)$, one can obtain the Z' rate for decays into charged-Higgs pairs [48]

$$\Gamma(Z' \to H^+H^-) = \frac{g'^2}{48\pi}(Q'_1\sin^2\beta - Q'_2\cos^2\beta)^2 m_{Z'}\left(1 - 4\frac{m_{H^\pm}^2}{m_{Z'}^2}\right)^{3/2} \tag{42}$$

and associated production of a W boson with a charged Higgs[9]

$$\Gamma(Z' \to W^\pm H^\mp)$$
$$= \frac{g'^2}{48\pi}(Q'_1 + Q'_2)^2 m_{Z'}\sin^2\beta\cos^2\beta\left[1 + 2\frac{5m_W^2 - m_{H^\pm}^2}{m_{Z'}^2} + \frac{(m_W^2 - m_{H^\pm}^2)^2}{m_{Z'}^4}\right]$$
$$\times \sqrt{1 - 2\frac{m_W^2 + m_{H^\pm}^2}{m_{Z'}^2} + \frac{(m_W^2 - m_{H^\pm}^2)^2}{m_{Z'}^4}}. \tag{43}$$

As the Z' has no direct coupling with W's, the decay into W^+W^- pairs occurs by means of the Z–Z' mixture. For small values of the Z–Z' mixing angle, this width reads [48]:

$$\Gamma(Z' \to W^+W^-) = \frac{g'^2}{48\pi}(Q'_1\cos^2\beta - Q'_2\sin^2\beta)^2 m_{Z'}. \tag{44}$$

In order to obtain the widths into Z-Higgs pairs, i.e. Zh, ZH or ZH' final states, or into scalar–pseudoscalar neutral-Higgs pairs, such as hA, HA or $H'A$, one first needs to diagonalize the neutral Higgs mass matrix (see [12]). The Z-Higgs rate can be written in compact form as:

$$\Gamma(Z' \to Zh_i)$$
$$= \frac{g'^2}{48\pi}(Q'_1\cos\beta U_{1i} - Q'_2\sin\beta U_{2i})^2 m_{Z'}\left[1 + 2\frac{5m_Z^2 - m_{h_i}^2}{m_{Z'}^2} + \frac{(m_W^2 - m_{h_i}^2)^2}{m_{Z'}^4}\right]$$
$$\times \sqrt{1 - 2\frac{m_Z^2 + m_{h_i}^2}{m_{Z'}^2} + \frac{(m_W^2 - m_{h_i}^2)^2}{m_{Z'}^4}}, \tag{45}$$

where $i = 1, 2, 3$ for final states Zh, ZH and ZH', respectively, and U_{ij} is the matrix which diagonalizes the Higgs mass matrix in the $(h \ H \ H')$ basis. Likewise, using the same notation as in Eq. (45), the scalar–pseudoscalar Higgs width reads:

---

[9] Eq. (43) corrects a typing mistake present in Ref. [12], wherein the decay width $Z' \to W^\pm H^\mp$ is instead 4 times smaller than in (43).

$$\Gamma(Z' \to h_i A) = \frac{g'^2}{48\pi} \frac{v^2}{N^2} \left(v_3 Q_1' \sin\beta U_{1i} + v_3 Q_2' \cos\beta U_{2i} + v Q_3' \sin\beta \cos\beta U_{3i} \right)^2 m_{Z'}$$
$$\times \left[1 - 2\frac{m_{h_i}^2 + m_A^2}{m_{Z'}^2} + \frac{(m_{h_i}^2 - m_A^2)^2}{m_{Z'}^4} \right]^{3/2}. \tag{46}$$

In Eq. (46), following [12], we defined $N = \sqrt{v_1^2 v_2^2 + v_1^2 v_3^2 + v_2^2 v_3^2}$ and $v = \sqrt{v_1^2 + v_2^2}$.

Finally, one can derive the decay widths into gauginos. As for neutralinos, after diagonalizing the mass matrix (21), the interaction Lagrangian reads:

$$\mathscr{L}_{\tilde{\chi}^0} = \sum_{i,j} g_{ij} \overline{\tilde{\chi}}_i^0 \gamma^\mu \gamma_5 \tilde{\chi}_j^0 Z_\mu', \tag{47}$$

where g_{ij} is a generalized coupling depending on the diagonalizing-matrix elements and has been calculated numerically. The partial rate into neutralino pairs $(\tilde{\chi}_i^0 \tilde{\chi}_j^0)$ with masses m_i and m_j is thus given by:

$$\Gamma(Z' \to \tilde{\chi}_i^0 \tilde{\chi}_j^0) = \frac{g_{ij}^2}{12\pi} m_{Z'} \left[1 - \frac{m_i^2 + m_j^2}{2m_{Z'}^2} - \frac{(m_i^2 - m_j^2)^2}{2m_{Z'}^4} - 3\frac{m_i m_j}{m_{Z'}^2} \right]$$
$$\times \sqrt{ \left[1 - \frac{(m_i + m_j)^2}{m_{Z'}^2} \right] \left[1 - \frac{(m_i - m_j)^2}{m_{Z'}^2} \right] }. \tag{48}$$

Finally, the Lagrangian term corresponding to the coupling of the Z' with charginos is given by:

$$\mathscr{L}_{\tilde{\chi}^\pm} = \frac{g'}{2} \sum_{i,j} \overline{\tilde{\chi}}_i^\pm \gamma^\mu (v_{ij} + a_{ij}\gamma_5) \tilde{\chi}_j^\pm Z_\mu'. \tag{49}$$

The generalized vector and vector-axial couplings can be expressed in terms of $\phi_\pm$, the angles of the unitary transformation diagonalizing the chargino mass matrix [18], and the Higgs U(1)' charges as follows [12]:

$$v_{11} = Q_1' \sin^2\phi_- - Q_2' \sin^2\phi_+,$$
$$a_{11} = Q_1' \sin^2\phi_- + Q_2' \sin^2\phi_+,$$
$$v_{12} = v_{21} = Q_1' \sin^2\phi_- \cos\phi_- - \delta Q_2' \sin\phi_+ + \cos\phi_+,$$
$$a_{12} = a_{21} = Q_1' \sin^2\phi_- \cos\phi_+ + \delta Q_2' \sin\phi_+ + \cos\phi_+,$$
$$v_{22} = Q_1' \cos^2\phi_- - Q_2' \cos^2\phi_+,$$
$$a_{22} = Q_1' \cos^2\phi_- + Q_2' \cos^2\phi_+. \tag{50}$$

In the above equations, $\delta = \mathrm{sgn}(m_{\tilde{\chi}_1^\pm})\mathrm{sgn}(m_{\tilde{\chi}_2^\pm})$. The analytical expressions for $\phi_\pm$ can be found in [18] and are not reported here for brevity. The rate into chargino pairs is finally given by:

$$\Gamma(Z' \to \tilde{\chi}_i^\pm \tilde{\chi}_j^\mp) = \frac{g'^2}{48\pi} m_{Z'} \left\{ (v_{ij}^2 + a_{ij}^2) \left[1 - \frac{m_i^2 + m_j^2}{2m_{Z'}^2} - \frac{(m_i^2 - m_j^2)^2}{2m_{Z'}^4} \right] \right.$$
$$\left. - 3(v_{ij} - a_{ij})^2 \frac{m_i m_j}{m_{Z'}^2} \right\}$$
$$\times \sqrt{ \left[1 - \frac{(m_i + m_j)^2}{m_{Z'}^2} \right] \left[1 - \frac{(m_i - m_j)^2}{m_{Z'}^2} \right] }. \tag{51}$$

References

 [1] P. Langacker, Rev. Mod. Phys. 81 (2009) 1199.
 [2] J.L. Hewett, T.G. Rizzo, Phys. Rep. 183 (1989) 193.
 [3] E. Salvioni, G. Villadoro, F. Zwirner, JHEP 0911 (2009) 068.
 [4] E. Salvioni, A. Strumia, F. Zwirner, JHEP 1003 (2010) 010.
 [5] CDF Collaboration, Phys. Rev. Lett. 106 (2011) 121801.
 [6] D0 Collaboration, Phys. Lett. B 695 (2011) 88.
 [7] ATLAS Collaboration, Phys. Rev. Lett. 107 (2011) 272002;
     ATLAS Collaboration, Phys. Lett. B 700 (2011) 163.
 [8] CMS Collaboration, JHEP 1105 (2011) 093.
 [9] L. Randall, R. Sundrum, Phys. Rev. Lett. 83 (1999) 4690.
[10] H.E. Haber, G.L. Kane, Phys. Rep. 117 (1985) 75.
[11] R. Barbieri, S. Ferrara, C.A. Savoy, Phys. Lett. B 119 (1982) 343.
[12] T. Gherghetta, T.A. Kaeding, G.L. Kane, Phys. Rev. D 57 (1998) 3178. See also the unpublished version, arXiv:hep-ph/9701343v2, for the complete expressions of mass matrices and decay widths.
[13] J. Kang, P. Langacker, Phys. Rev. D 71 (2005) 035014.
[14] V. Barger, P. Langacker, H.-S. Lee, G. Shaughnessy, Phys. Rev. D 73 (2006) 115010.
[15] V. Barger, P. Langacker, G. Shaughnessy, Phys. Lett. B 644 (2007) 361.
[16] M. Baumgart, T. Hartman, C. Kilic, L.-T. Wang, JHEP 0711 (2007) 084.
[17] C.-F. Chang, K. Cheung, T.-C. Yuan, JHEP 1109 (2011) 058.
[18] S.P. Martin, A supersymmetry primer, in: G.L. Kane (Ed.), Perspectives on Supersymmetry II, pp. 1–153, arXiv:hep-ph/9709356.
[19] B. de Carlos, J. Espinosa, Phys. Lett. B 407 (1997) 12.
[20] J. Kalinowski, S.F. King, J.P. Roberts, JHEP 0901 (2009) 066.
[21] G. Bélanger, J. Da Silva, A. Pukhov, JCAP 1112 (2011) 014.
[22] G. Corcella, et al., JHEP 0101 (2001) 010;
     S. Gieseke, et al., arXiv:1102.1672 [hep-ph].
[23] T. Sjostrand, S. Mrenna, P. Skands, JHEP 0605 (2006) 026;
     T. Sjostrand, S. Mrenna, P. Skands, Comput. Phys. Commun. 178 (2008) 852.
[24] J. Erler, P. Langacker, T. Li, Phys. Rev. D 66 (2002) 015002.
[25] E. Nardi, Phys. Rev. D 48 (1993) 3277.
[26] E. Nardi, Phys. Rev. D 49 (1994) 4394.
[27] E. Nardi, T.G. Rizzo, Phys. Rev. D 50 (1994) 203.
[28] R.W. Robinett, J.L. Rosner, Phys. Rev. D 25 (1982) 3036;
     R.W. Robinett, J.L. Rosner, Phys. Rev. D 27 (1983) 679 (Erratum).
[29] J. Erler, P. Langacker, S. Munir, E. Rojas, JHEP 0908 (2009) 017.
[30] K.S. Babu, C. Kolda, J. March-Russell, Phys. Rev. D 54 (1996) 4635.
[31] V. Barger, K. Whisnant, Int. J. Mod. Phys. A 3 (1988) 1907.
[32] S. Nandi, Phys. Lett. 197 (1997) 144.
[33] P. Fayet, J. Iliopoulos, Phys. Lett. B 51 (1974) 461.
[34] L. O'Raifeartaigh, Nucl. Phys. B 96 (1975) 331.
[35] K. Nakamura, et al., J. Phys. G 37 (2010) 075021.
[36] DELPHI Collaboration, ALEPH Collaboration, L3 Collaboration, OPAL Collaboration, LEP Working Group for Higgs Boson Searches, Phys. Lett. B 565 (2003) 61.
[37] CDF Collaboration, D0 Collaboration, Phys. Rev. Lett. 104 (2010) 061802;
     CDF Collaboration, D0 Collaboration, Phys. Rev. Lett. 109 (2012) 071804.
[38] ATLAS Collaboration, Phys. Lett. B 710 (2012) 49;
     ATLAS Collaboration, Phys. Rev. D 86 (2012) 032003.
[39] CMS Collaboration, Phys. Lett. B 710 (2012) 26;
     CMS Collaboration, Phys. Lett. B 716 (2012) 30.
[40] F.E. Paige, S.D. Protopopescu, H. Baer, X. Tata, hep-ph/0312045.
[41] J. Pumplin, D.R. Stump, J. Huston, H.L. Lai, P. Nadolsky, W.K. Tung, JHEP 0207 (2002) 012.
[42] R. Hamberg, W.L. van Neerven, T. Matsuura, Nucl. Phys. B 359 (1991) 343;
     R. Hamberg, W.L. van Neerven, T. Matsuura, Nucl. Phys. B 644 (2002) 403 (Erratum).
[43] R.V. Harlander, W.B. Kilgore, Phys. Rev. Lett. 88 (2002) 201801.

[44] J. Erler, P. Langacker, S. Munir, E. Rojas, JHEP 1111 (2011) 076.
[45] C.-W. Chiang, N.D. Christensen, G.-J. Ding, T. Han, Phys. Rev. D 85 (2012) 015023.
[46] M.L. Mangano, M. Moretti, F. Piccinini, R. Pittau, A. Polosa, JHEP 0307 (2003) 001.
[47] R. Gavin, Y. Li, F. Petriello, S. Quackenbush, Comput. Phys. Commun. 182 (2011) 2388.
[48] N.G. Deshpande, J. Trampetic, Phys. Lett. B 206 (1988) 665.